Heme−Peptide Models for Hemoproteins. 1. Solution Chemistry of *N*-Acetylmicroperoxidase-8

Orde Q. Munro*,[1a] and Helder M. Marques[1b]

Centre for Molecular Design, Department of Chemistry, University of the Witwatersrand, Wits 2050, Johannesburg, South Africa

Received March 8, 1995[⊗]

An improved method for the preparation of the heme octapeptide acetyl-MP8, obtained by proteolysis of horse heart cytochrome *c*, is described. AcMP8 obeys Beer's law at pH 7.0 in aqueous solution up to a concentration of 3×10^{-5} M. The self-association constant measured at 25 °C ($\log K_D = 4.04$) is an order of magnitude lower than that for MP8, reflecting the role of the *N*-acetyl protecting group in abolishing intermolecular coordination. However, AcMP8 does form π-stacked dimers in aqueous solution with increasing ionic strength. A more weakly packed $\pi-\pi$ dimer reaches a maximum abundance at ~3 M ionic strength, but a more tightly packed dimer is favored at $\mu > 3$ M. An equilibrium model based on charge neutralization by specific binding of Na^+ ions gives a total molecular charge of 3− for AcMP8 at pH 7.0 and a self-association constant $\log K_D = 4.20$. AcMP8 exhibits six spectroscopically active pH-dependent transitions. The Glu-21 *c*-terminal carboxylate binds to the heme iron at low pH ($pK_a = 2.1$) but is substituted by His-18 ($pK_a = 3.12$) as the pH increases. The two heme propanoic acid substituents ionize with pK_a's of 4.95 and 6.1. This is followed by ionization of iron-bound water with a $pK_a = 9.59$, $\Delta H = 48 \pm 1$ kJ mol^{-1}, and $\Delta S = -22 \pm 3$ J K^{-1} mol^{-1}. The electronic spectra indicate that AcMP8 is predominantly in the $S = {}^5/_2$ state at pH 7.0, while the hydroxo complex at pH 10.5 corresponds to an equilibrium mixture of $S = {}^5/_2$ and $S = {}^1/_2$ states at 25 °C. In the final transition, His-18 ionizes to form the $S = {}^1/_2$ histidin*ate* complex with a pK_a of 12.71. AcMP8 is relatively stable under alkaline conditions, dimerizing slowly at high pH ($k = 2.59 \pm 0.14$ M^{-1} s^{-1}) to form a high-spin μ-oxo-bridged species. The pH-dependent behavior of AcMP8 in the presence of excess 3-cyanopyridine, however, is markedly different. At low pH, AcMP8 simultaneously binds the exogenous ligand and the Glu-21 *c*-terminal carboxylate with a $pK_a < 2$. His-18 replaces the carboxylate ligand at higher pH ($pK_a = 2.60$), and both heme propanoic acid groups ionize with a mean $pK_a = 5.10$. Unlike AcMP8···OH$^-$, the axial histidine of the 3-CNPy complex ionizes at near neutral pH ($pK_a = 7.83$), prior to being replaced by OH$^-$ ($pK_a = 10.13$). The sixth transition in the AcMP8/3-CNPy system produces the bis(hydroxo) complex ($pK_a > 13$).

Introduction

Hemoproteins, such as myoglobin, cytochrome *c* peroxidase, many plant peroxidases, and cytochrome *c*′, exhibit axial coordination of the heme group by a single histidyl residue from the protein.[1c,d] A biomimetic analog for these hemoproteins should therefore support an appended imidazole base that can compete effectively for one of the coordination sites at the metal in the presence of solvent and exogenous ligands.[2−5] One of the main complications encountered with simple biomimetic systems, for example $[M(PPIX)]^{n+}$,[6] $[M(OEP)]^{n+}$, and $[M(TPP)]^{n+}$ species, is their low solubility in aqueous solution. Physical studies on such systems have therefore depended on the use of organic solvents, mixed solvents, and detergents to circumvent aggregation.[7] In fact, the propensity of simple metalloporphyrins, including those with appended solubilizing groups,[8] to aggregate at fairly low concentrations in aqueous solution[9,10] and the difficulty of preparing mixed-ligand complexes[11] have frequently compromised[12] the application of such

⊗ Abstract published in *Advance ACS Abstracts,* May 1, 1996.

(1) (a) Current address: Department of Chemistry and Biochemistry, University of Notre Dame, Notre Dame, IN 46556. Electronic mail: munro.1@nd.edu. (b) Electronic mail: hmarques@aurum.chem.wits.ac.za. (c) Hughes, M. N. In *Comprehensive Coordination Chemistry* Wilkinson, G., Ed.; Pergamon Press: Oxford, U.K., Vol. 6. 1987; (d) *Metalloproteins: Chemical Properties and Biological Effects*; Otsuka, S., Yamanaka, T., Eds.; Elsevier: Amsterdam, 1988.

(2) Morgan, B.; Dolphin, D. *Struct. Bonding* **1987**, *64*, 115.

(3) Meunier, B.; de Carvalho, M. E.; Bortoloni, O.; Momenteau, M. *Inorg. Chem.* **1988**, *27*, 161.

(4) Belal, R.; Momenteau, M.; Meunier, B. *J. Chem. Soc., Chem. Commun.* **1989**, 412.

(5) Momenteau, M.; Loock, B.; Huel, C.; Lhoste, J. M. *J. Chem. Soc., Perkin Trans. 1* **1988**, 283.

(6) Abbreviations: AcMP8, *N*-acetylmicroperoxidase-8; CHES, 2-(cyclohexylamino)ethanesulfonic acid; 3-CNPy, 3-cyanopyridine; CT, charge-transfer; EDC, *N*-(3-(dimethylamino)propyl)-*N*′-ethylcarbodiimide hydrochloride; Hb, hemoglobin; HHis, neutral histidine; His$^-$, anionic histidine (histidin*ate*); HIm, neutral imidazole; L, general ligand; M, metal ion; Mb, myoglobin; 1-MeIm, 1-methylimidazole; 4(5)-MeHIm, 4(5)-methylimidazole; MES, 2-(morpholino)ethanesulfonic acid; MOPS, 3-(-morpholino)propanesulfonic acid; MP11, microperoxidase-11; MP9, microperoxidase-9; MP8, microperoxidase-8; MP6, microperoxidase-6; *c*-Mu, *cis*-methyl urocanate; *t*-Mu, *trans*-methyl urocanate; OEP, 2,3,7,8,12,13,17,18-octaethylporphyrin; PPIX, protoporphyrin IX; PPIXDME, protoporphyrin IX dimethyl ester; RP, reverse-phase (C-18); TMPyP, 5,10,15,20-tetrakis(*N*-methylpyridiniumyl)porphyrin; TPP, 5,10,15,20-tetraphenylporphyrin; Tris, tris(hydroxymethyl)aminomethane; UroP, uroporphyrin.

(7) (a) White, W. I. In *The Porphyrins*; Dolphin, D., Ed.; Academic Press: New York, 1978; Vol. V. Chapter 7. (b) White, W. I.; Plane, R. A. *Bioinorg. Chem.* **1974**, *4*, 21. (c) Simplicio, J.; Schwenzer, K. *Biochemistry* **1973**, *12*, 1923. (d) Hambright, P.; Chock, P. B. *J. Inorg. Nucl. Chem.* **1975**, *37*, 2363. (e) Simplicio, J. *Biochemistry* **1972**, *11*, 2525. (f) Maehly, M. C.; Åkeson, A. *Acta Chem. Scand.* **1958**, *12*, 1259. (g) Davies, T. H. *Biochim. Biophys. Acta* **1973**, *329*, 108. (h) Patel, M. J.; Kassner, R. J. *Biochem. J.* **1989**, *262*, 959.

(8) (a) Pasternack, R. F.; Huber, P. R.; Boyd, P.; Engasser, G.; Francesconi, L.; Gibbs, E.; Fasella, P.; Venturo, G. C.; de Hinds, L. C. *J. Am. Chem. Soc.* **1972**, *94*, 4511. (b) Pasternack, R. F. *Ann. N.Y. Acad. Sci.* **1973**, *206*, 614.

(9) (a) Gallagher, W. A.; Elliot, W. B. *Ann N.Y. Acad. Sci.* **1973**, *206*, 463. (b) Brown, S. R.; Hatzikonstantinou, H.; Herries, D. G. *Int. J. Biochem.* **1980**, *12*, 701. (c) Brown, S. B.; Dean, T. C.; Jones, P. *Biochem. J.* **1970**, *117*, 733.

S0020-1669(95)00284-9 CCC: $12.00

systems in biomimetic studies. Simple iron porphyrins do, however, fulfill an important role in the delineation of factors that control the electronic properties of the metal ion and have undoubtedly contributed to our fundamental understanding of the electronic,[13] Mössbauer,[14] magnetic,[15] EPR,[16] and structural[17] properties of the prosthetic groups of hemoproteins.

An attractive alternative to synthetic iron porphyrins is the range of heme−peptide fragments that may be obtained proteolytically from cytochrome *c*. These fragments are *water-soluble* and can be prepared with different numbers of amino acid residues comprising the polypeptide chain appended to the heme group.[18] Furthermore, since all retain the proximal histidine of the parent cytochrome as a ligand to the heme iron,[19a] mixed axial ligation of the metal in the heme−peptide fragment is inherently feasible.[19b] The nomenclature used to describe these heme−peptide fragments (microperoxidases) is shown in Figure 1.

Although these species are soluble over a wide range of pH and temperature, they do aggregate in aqueous solution by two principal mechanisms: (i) concentration-dependent intermolecular coordination,[19a,20] wherein free amino groups of the peptide chain compete for the axial coordination site *trans* to His-18, and (ii) noncovalent π-interactions between the more exposed distal faces of two or more heme peptides.[21,22]

Sequential peptic and tryptic hydrolysis of cytochrome *c* is used to prepare MP8 (Figure 1),[23] perhaps the most thoroughly studied of the microperoxidases. Electronic,[24,25] CD,[22] NMR,[26] and EPR[27,28] data for MP8 indicate that $\pi-\pi$ aggregation as

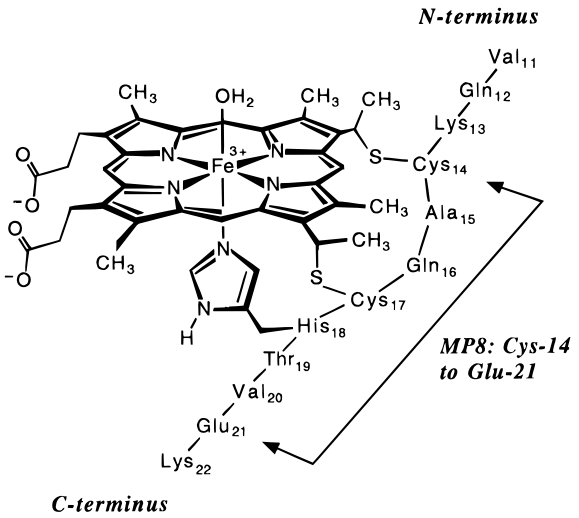

Figure 1. The heme−peptide fragments, depicted as six-coordinate aqua complexes, that are obtained by selective proteolysis of cytochrome *c*. The amino acid sequence of the polypeptide chain is numbered according to that in horse heart cytochrome *c*[19a] and determines the nomenclature of the corresponding microperoxidase fragments: MP6, Cys-14 to Thr-19; MP8, Cys-14 to Glu-21; MP9, Cys-14 to Lys-22; MP11, Val-11 to Glu-21.

well as intermolecular coordination *via* the α-amino group of Cys-14 occurs. Monomeric solutions of MP8 for kinetic,[29] thermodynamic,[29,30] redox,[31] and magnetic[32] studies have depended on the use of solvent mixtures or added ligands to disperse aggregates. The systematic work of Aron *et al.*,[33] however, showed that studies at very high dilution in pure water were feasible, and monomeric MP8 has, as a result, been used to model the high-valent iron−oxo intermediates that are known to occur in the catalytic cycles of the peroxidases and catalases.[34−36]

The reaction of MP8 (Figure 1) with acetic anhydride selectively protects the α-amino group of Cys-14, affording AcMP8.[37] Yang and Sauer[37] reported optical and magnetic properties of some complexes of both MP8 and AcMP8; although this work concentrated on the *N*-acetylmethionine complex of AcMP8, there is evidence from their EPR data that the *N*-acetyl group of the heme peptide eliminates dimerization by blocking intermolecular coordination. The pH at which many of the experiments were carried out, however, appears not to have been reported, and this complicates interpretation of the

(10) (a) Satterlee, J. D.; Shelnutt, J. A. *J. Phys. Chem.* **1984**, *88*, 5487. (b) Shelnutt, J. A.; Dobry, M. M.; Satterlee, J. D. *J. Phys. Chem.* **1984**, *88*, 4980. (c) Satterlee, J. D.; Shelnutt, J. A. *Inorg. Chim. Acta* **1985**, *106*, 165. (d) Pasternack, R. F.; Francesconi, L.; Raff, D.; Spiro, E. *Inorg. Chem.* **1973**, *12*, 2606.
(11) Marques, H. M. *Inorg. Chim. Acta* **1991**, *190*, 291.
(12) (a) Graf, W.; Blanck, J.; Scheler, W. *Acta Biol. Med. Ger., Suppl.* **1964**, *3*, 93. (b) Graf, W.; Pommerening, K.; Scheler, W. *Acta Biol. Med. Ger.* **1971**, *26*, 895. (c) Cowghill, R. W.; Clark, W. M. *J. Biol. Chem.* **1952**, *198*, 33. (d) Davies, T. H. *J. Biol. Chem.* **1940**, *135*, 597.
(13) (a) Loew, G. H. In *Iron Porphyrins, Part 1*; Lever, A. B. P., Gray, H. B., Eds.; Physical Bioinorganic Chemistry Series; Addison-Wesley: Reading, MA, 1983; p 1. (b) Makinen, M. W.; Churg, A. K. In *Iron Porphyrins, Part 1*; Lever, A. B. P., Gray, H. B., Eds.; Physical Bioinorganic Chemistry Series; Addison-Wesley: Reading, MA, 1983; p 141. (c) Dawson, J. H.; Dooley, D. M. In *Iron Porphyrins, Part 3*; Lever, A. B. P., Gray, H. B., Eds.; Physical Bioinorganic Chemistry Series; VCH Publishers: New York, 1989; p 1. (d) Eaton, W. A.; Hofrichter, J. In *Methods in Enzymology*; Antonini, E., Rossi-Barnardi, L., Chiancone, E., Eds.; Academic Press: New York, 1981; Vol. 76, p 175.
(14) Debrunner, P. G. In *Iron Porphyrins, Part 3*; Lever, A. B. P., Gray, H. B., Eds.; Physical Bioinorganic Chemistry Series; VCH Publishers: New York, 1989; p 137.
(15) Mitra, S. In *Iron Porphyrins, Part 2*; Lever, A. B. P., Gray, H. B., Eds.; Physical Bioinorganic Chemistry Series; Addison-Wesley: Reading, MA, 1983; p 1.
(16) Palmer, G. In *Iron Porphyrins, Part 2*; Lever, A. B. P., Gray, H. B., Eds.; Physical Bioinorganic Chemistry Series; Addison-Wesley: Reading, MA, 1983; p 43.
(17) Scheidt, W. R.; Lee, Y. J. *Struct. Bonding* **1987**, *64*, 1.
(18) (a) Tsou, C. L. *Nature* **1949**, *164*, 1134. (b) Tsou, C. L. *Biochem. J.* **1951**, *49*, 362. (c) Tsou, C. L. *Biochem. J.* **1951**, *49*, 367.
(19) (a) Paléus, S.; Ehrenberg, A.; Tuppy, H. *Acta Chem. Scand.* **1955**, *9*, 365. (b) Hamza, M. S. A.; Pratt, J. M. *J. Chem. Soc., Dalton Trans.* **1994**, 1367.
(20) Ehrenberg, A.; Theorell, H. *Acta Chem. Scand.* **1955**, *9*, 1193.
(21) Urry, D. W. *J. Am. Chem. Soc.* **1967**, *89*, 4190.
(22) Urry, D. W.; Pettegrew, J. W. *J. Am. Chem. Soc.* **1967**, *89*, 5276.
(23) Tuppy, H.; Paléus, S. *Acta Chem. Scand.* **1955**, *9*, 353.
(24) Harbury, H. A.; Loach, P. A. *Proc. Natl. Acad. Sci. U.S.A.* **1959**, *45*, 1344.
(25) Harbury, H. A.; Loach, P. A. *J. Biol. Chem.* **1960**, *235*, 2646.
(26) Smith, M. C.; McLendon, G. *J. Am. Chem. Soc.* **1981**, *103*, 4912.
(27) Hamilton, G. J.; Owens, J. W.; O'Connor, C. J.; Kassner, R. J. *Inorg. Chim. Acta* **1984**, *93*, 55.
(28) Owens, J. W.; O'Connor, C. J. *Inorg. Chim. Acta* **1988**, *151*, 107.
(29) (a) Smith, M. C.; McLendon, G. *J. Am. Chem. Soc.* **1980**, *102*, 5666. (b) Huang, Y.-P.; Kassner, R. J. *J. Biol. Chem.* **1981**, *256*, 5327. (c) Blumenthal, D. C.; Kassner, R. J. *J. Biol. Chem.* **1979**, *254*, 9617. (d) Blumenthal, D. C.; Kassner, R. J. *J. Biol. Chem.* **1980**, *255*, 5859. (e) Marques, H. M.; Baldwin, D. A.; Pratt, J. M. *J. Inorg. Biochem.* **1987**, *29*, 77. (f) Marques, H. M.; Baldwin, D. A.; Pratt, J. M. *S. Afr. J. Chem.* **1988**, *41*, 68.
(30) Byfield, M. P.; Pratt, J. M. *J. Chem. Soc., Chem. Commun.* **1992**, 214.
(31) (a) McLendon, G.; Smith, M. *Inorg. Chem.* **1982**, *21*, 847. (b) Myer, Y. P.; Harbury, H. A. *Ann. N.Y. Acad. Sci.* **1973**, *206*, 685.
(32) (a) Huang, Y.-P.; Kassner, R. J. *J. Am. Chem. Soc.* **1981**, *103*, 4927. (b) Huang, Y.-P.; Kassner, R. J. *J. Am. Chem. Soc.* **1979**, *101*, 5807.
(33) Aron, J.; Baldwin, D. A.; Marques, H. M.; Pratt, J. M.; Adams, P. A. *J. Inorg. Biochem.*, **1986**, *27*, 227−243.
(34) (a) Baldwin, D. A.; Marques, H. M.; Pratt, J. M. *J. Inorg. Biochem.* **1987**, *30*, 203. (b) Adams, P. A.; Goold, R. D. *J. Chem. Soc., Chem. Commun.* **1990**, 97. (c) Adams, P. A. *J. Chem. Soc., Perkin Trans. 2* **1990**, 1407.
(35) Cunningham, I. D.; Bachelor, J. L.; Pratt, J. M. *J. Chem. Soc., Perkin Trans. 2* **1991**, 1839.
(36) Balch, A. L. *Inorg. Chim. Acta* **1992**, *198*−200, 297.
(37) Yang, E. K.; Sauer, K. In *Electron Transport and Oxygen Utilization*; Ho, C., Ed.; Elsevier: Amsterdam, 1982; p 82.

results. Definitive evidence for acetylation of the Cys-14 α-amino group of MP8 is therefore lacking.

AcMP8 was also recently[38] used in low-temperature kinetic studies to model compounds **O**, **I**, and **II** of the catalytic cycle of the peroxidases. While part of the current work was in progress, Wang *et al.*[39] reported resonance Raman, EPR, and solution studies on AcMP8 and some of its complexes with anionic ligands. In this and a previous report,[40] they concluded that, at ambient temperature and neutral pH, AcMP8 exists in a *thermal* equilibrium between *pure* $S = {}^5/_2$ and $S = {}^3/_2$ species.

The present article concerns delineation of the solution behavior of AcMP8 and provides the ground work on which further physical studies on this system are based. In part 2[41a] we have used molecular exciton theory[41b] to determine possible structures for the AcMP8 π-stacked dimers that are formed with increasing ionic strength in aqueous solution. Mössbauer, EPR, and magnetic susceptibility measurements on the heme peptide are presented in parts 3[41c] and 4[41d] as a function of pH and temperature and demonstrate that the unique pH-dependent forms of AcMP8 are best described as thermal spin-equilibrium mixtures of a quantum-mechanically admixed intermediate-spin ($S = {}^3/_2$, ${}^5/_2$) and low-spin ($S = {}^1/_2$) species.

Experimental Section

Water was twice distilled in an all-glass Buchi Fontavapor 285 still and further purified by a Milli-Q system (18 MΩ cm). All pH measurements were made with a Metrohm Series 6.0216 combination glass microelectrode and a Metrohm 605 pH meter. Calibration was performed against primary standard buffers.[42] Spectroscopic work was performed on either a Cary 2300 or a Cary 1E spectrophotometer with a wavelength accuracy of ±0.2 nm. Cell turrets were thermostated at 25.0 ± 0.2 °C, and to the same accuracy at other temperatures. The concentrations of AcMP8 solutions for optical spectroscopy were determined at pH 7.0 (50 mM MOPS, $\mu = 0.10$ M (KCl), 25 °C) using the same molar absorptivity for AcMP8 as that determined for monomeric MP8.[33] Data were analyzed by conventional linear or by nonlinear least-squares numerical methods.

Analytical HPLC was performed on a Spherisorb S5 ODS2 (15 cm × 4.6 mm) analytical column using a SpectraPhysics 8800 ternary gradient pump, a Linear UVis 200 detector (set at 400 nm), and a Varian 4290 integrator. Samples (20 μL) were injected onto the column at equilibrium with the initial solvent composition of 100% A (50 mM phosphate buffer at pH 6.75). Elution was effected at 2.5 mL min^{-1} with a linear gradient resulting in 80% A, 20% B (acetonitrile) at $t =$ 10 min; this composition was maintained until $t = 12$ min, before commencing a linear return to the starting composition at $t = 14$ min. Semipreparative HPLC work, when required, was performed with the above instrument at a flow rate of 7.50 mL min^{-1} on a Brownlee C-18 column (250 × 10 mm, 20 μm) using 500 μL injection volumes, commencing with 80% A (50 mM phosphate buffer at pH 3.0), 20% B and progressing linearly to 60% A, 40% B at $t = 10$ min; the isocratic phase and return to the starting composition were as above. Columns were purged with 50% aqueous acetonitrile daily in an attempt to eliminate the build-up of heme-containing material. However, retention times were found to slowly increase with the age of the column packing.

Preparation of AcMP8. Published procedures[43,44] were used to prepare MP8 from equine cytochrome *c* (Servac, Cape Town, S. Africa) using porcine pepsin and trypsin (Sigma). MP8 was separated from residual MP11 and further hydrolysis products by chromatography on a column (3 × 40 cm) of Sephadex G50 (Pharmacia) using 0.1 M NH_4HCO_3 buffer (BDH) at a flow rate of 10 mL h^{-1}. Fractions containing ≥98% MP8 were pooled, and the solution was desalted by five successive concentration/dilution steps in an Amicon cell (50 mL) using a YM2 Duraflo membrane operating at 70 psi. Lyophilization afforded solid MP8. Acetylation was accomplished by dissolving solid MP8 (∼25 mg) in 6 mL of 0.2 M pH 9.3 sodium carbonate (BDH) buffer, prior to cooling the solution to 4 °C and injecting a 500 molar excess of acetic anhydride (Merck). The reaction mixture was allowed to heat to 30 °C at the heating rate of the thermostatic bath (∼25 min) and maintained at this temperature for 3 h. Analysis of the reaction mixture by HPLC using authentic MP8 spikes (Sigma) revealed close to 100% conversion of MP8 to AcMP8 after 3 h. Production of acetic acid during acetylation shifted the pH to ∼4, thereby inducing precipitation of AcMP8. Saturated ammonium sulfate solution was added dropwise to maintain the precipitate, and the mixture was centrifuged at 6000 rpm for 40 min. The supernatant was discarded, the solid dissolved in dilute NaOH (∼10^{-5} M), and the solution desalted as before. This yielded ≥98% solid AcMP8 after lyophilization. Preparations which yielded <96% AcMP8 were further purified by semipreparative HPLC. For large-scale preparations of AcMP8 (∼200 mg), a concentrated slurry of MP8 in deionized water (∼8 mL) was produced by ultrafiltration (Amicon cell). The slurry was then dissolved in an equal volume of 0.4 M pH 9.3 $NaHCO_3$ buffer, the solution cooled to 4 °C, and the appropriate excess of acetic anhydride injected as before.

EDC-Coupled Reaction of AcMP8 with *n*-Propylamine. AcMP8 (5.4 mg) was dissolved in 2.50 mL of 0.013 M *n*-propylamine solution (BDH) at pH 4.74 (25 °C) and 2.5 mg of *N*-(3-(dimethylamino)propyl)-*N*′-ethylcarbodiimide hydrochloride (EDC, Sigma) added. The pH of the stirred solution climbed rapidly to ca. 4.9 prior to commencing a gradual return to ∼4.8 after 40 min. Analysis of a sample taken from the reaction mixture at $t = 30$ min by semipreparative HPLC (using the elution gradient described above, but with a 50 mM pH 6.5 phosphate buffer and flow rate of 6.5 mL min^{-1} on a new column) indicated incomplete conversion of AcMP8 (retention time = 3.1 min) to an initial product (26%) with a retention time of 3.84 min. Three further 2.5-mg additions of EDC were made ca. 70, 95, and 146 min after the start of the reaction. In addition to AcMP8 (15%) and the first product (61%), a second product (23%) with a retention time of 5.01 min was obtained after 150 min. Since the yield of the first product was considered maximal, the reaction products were separated and isolated by semipreparative HPLC. Pure fractions (98%) of the first product were pooled, diluted with deionized water, loaded onto a C-18 Sep-Pak cartridge (Millipore), desalted with 40 mL of deionized water, and eluted with a minimal volume of methanol. The methanolic solution of this product could be safely stored for several weeks at 4 °C.

Spectrophotometric Titrations. Spectroscopic pK_a's were determined by titrating 25.040 mL of a 3.1 μM solution of AcMP8 in a multicomponent buffer system containing ∼1.0 mM each of potassium hydrogen phthalate, MES, MOPS, TRIS, and CHES as the noncoordinating buffers at a total initial ionic strength of 0.10 M (KCl) in a thermostatic cell at the appropriate temperature. The pH was adjusted from ∼pH 6 to pH 13.5, or from ∼pH 8 to pH 1.6 (fresh solution), by diffusion of microscopic aliquots of concentrated aqueous HCl or NaOH into the solution from glass capillaries. At each pH, 5 mL of solution was pumped into a thermostated 2.0 cm path length quartz cuvette housed in the spectrometer turret and the absorbance at the applicable wavelength (397.2 nm) measured before returning the sample to the reaction mixture. This procedure was also used to titrate a 200-μL aliquot of the methanolic solution of the first HPLC-purified *n*-propylamide derivative of AcMP8 in 25.00 mL of buffer solution thermostated at 25 °C. Spectroscopic pK_a's of the 6-coordinate 3-cyanopyridine complex of AcMP8 (3.1 μM) were determined using the above method in an analogous multicomponent buffer system containing 0.30 M 3-cyanopyridine (∼98% complexation of AcMP8

(38) Wang, J.-S.; Baek, H. K.; Van Wart, H. E. *Biochem. Biophys. Res. Commun.* **1991**, *179*, 1320.
(39) Wang, J.-S.; Tsai, A.-L.; Heldt, J.; Palmer, G.; Van Wart, H. E. *J. Biol. Chem.* **1992**, *267*, 15310.
(40) Wang, J.-S.; Van Wart, H. E. *J. Phys. Chem.* **1989**, *93*, 7925.
(41) (a) Part 2: Munro, O. Q.; Marques, H. M. *Inorg. Chem*. **1996**, *35*, 0000. (b) McRae, E. G.; Kasha, M. *J. Chem. Phys.* **1958**, *28*, 721. (c) Part 3: Munro, O. Q.; Marques, H. M.; Pollak, H.; van Wyk, J. Manuscript in preparation. (d) Part 4: Munro, O. Q.; Marques, H. M.; de Wet, M.; Hill, H. A. O.; Battle, P. D. Manuscript in preparation.
(42) (a) *Biochemists' Handbook*; Long, C., Ed.; Spon: London, 1971. (b) Boyd, W. *J. Biol. Chem.* **1965**, *240*, 4097.
(43) Adams, P. A.; Byfield, M. P.; Milton, R. C. d. L.; Pratt, J. M. *J. Inorg. Biochem.* **1988**, *34*, 167.
(44) Adams, P. A.; Byfield, M. P.; Goold, R. D.; Thumser, A. E. *J. Inorg. Biochem.* **1989**, *37*, 55.

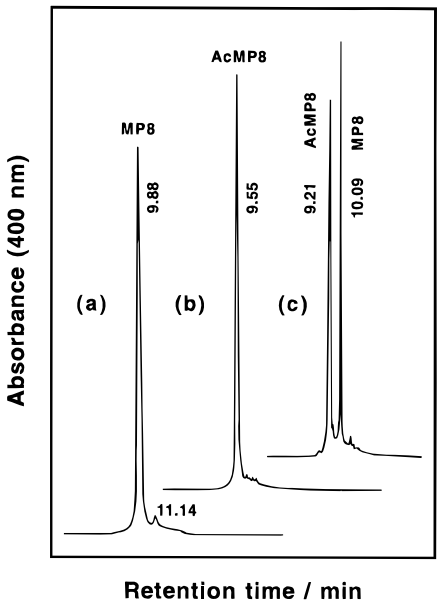

Figure 2. (a) Semipreparative-scale RP HPLC at pH 3.0 of a sample of MP8 (96%) obtained after tryptic hydrolysis of MP11 and purification on Sephadex G50. The product with a retention time of 11.14 min is MP6, which tends to coelute with the first few fractions of MP8 from Sephadex G50. (b) Analytical RP HPLC at pH 3.0 of a sample of AcMP8 (96%) produced after ∼2 h using the described method. (c) Analytical RP HPLC at pH 6.75 of the AcMP8 reaction product spiked with an authentic sample of MP8 (Sigma).

at pH 6.5). The absorbance at 397.2 and 403.0 nm was recorded as a function of the solution pH.

Ionic Strength Effects. Solid sodium perchlorate monohydrate (Merck) was added in fixed quantities (between 1 and 3 g) to 25.040 mL of a 3.1 μM solution of AcMP8 buffered at pH 7.00 (0.10 M MOPS initially, $\mu_i = 0.0386$ M) at 25 °C up to a total mass of ∼37 g. Absorbance changes with increasing ionic strength were measured as described for spectroscopic titrations. Addition of $NaClO_4 \cdot H_2O$ to the solution of AcMP8 effects a linear increase in the total volume. A correction curve for dilution effects was established by measuring the total solution volume (initially 25.0 mL) resulting from the addition of known quantities of $NaClO_4 \cdot H_2O$. The fitted function, $V_{tot} = 0.4879 \pm 0.0058m - 24.80 \pm 0.06$, where m is the mass of the added salt, was used to correct the measured values of $A_{397.2nm}$ and to calculate the total ionic strength of the solution at each point. Finally, UV spectra were collected as a function of ionic strength using separate solutions with [AcMP8] = 5.1 μM.

Results

Acetylation of MP8. In contrast to a previous report on the acetylation of MP11,[45] we found that reaction of MP8 with acetic anhydride at 4 °C (pH 9.3) failed to produce AcMP8 even after 14 h. The method developed here for the acetylation of MP8 affords ∼95% AcMP8 after only 25 min when starting from an initial temperature of 4 °C; retaining the reaction mixture at 30 °C results in cleaner conversion to AcMP8. Figure 2 shows the HPLC of a sample of AcMP8 produced after ∼2 h under the described conditions from MP8 (96%) and of the same sample spiked with authentic MP8 (Sigma) of approximately equal concentration.

Aggregation of AcMP8 in Aqueous Solution. An effective method for assessing concentration-dependent aggregation phenomena in solutions of metalloporphyrins is to determine the degree of adherence of the solution to Beer's law over the solute concentration range of interest.[7a] Deviation from Beer's law signals aggregation of the absorbing species, while a single set of isosbestic points reflect a simple equilibrium between two species.[8a] A Beer's law study of MP8 in aqueous phosphate buffer solution (pH 7.00, $\mu = 0.1$ M, 25 °C),[33] for example, revealed the existence of a simple monomer/dimer equilibrium (dimerization constant $K_D = (1.17 \pm 0.02) \times 10^5$ M^{-1}) below an MP8 concentration of 8.08×10^{-6} M but aggregation at concentrations above this. Since low-spin MP8 was obtained at the highest concentrations, this study suggested the likelihood of an aggregation mechanism involving intermolecular coordination by the Cys-14 α-amino group of MP8.[33]

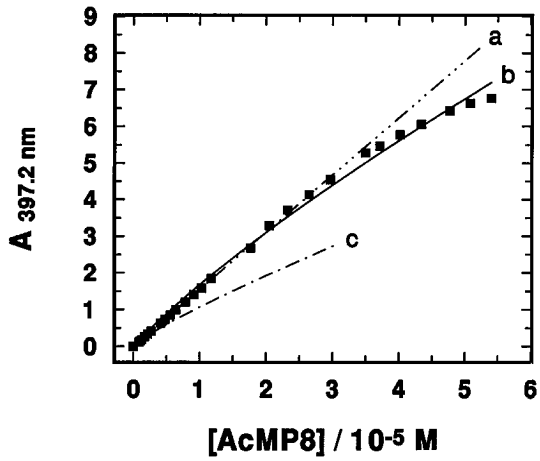

Figure 3. Beer's law plot for an aqueous solution of AcMP8 at pH 7.00 and at 25 °C (100 mM phosphate buffer, $\mu = 0.50$ M ($NaClO_4$)). The ordinate values are normalized for 10 mm path length cells. (a) The limiting slope at low [AcMP8]: $1.55 \pm 0.01 \times 10^5$ M^{-1} cm^{-1}. (b) The data fitted to eq 2, $K_D = 1.09 \pm 0.06 \times 10^4$ M^{-1}, $\epsilon_M = (1.88 \pm 0.02) \times 10^5$ M^{-1} cm^{-1}, and $\epsilon_D = (1.09 \pm 0.07) \times 10^5$ M^{-1} cm^{-1}. (c) The theoretical curve (eq 2) fitting the data for MP8 in aqueous solution.[43]

In aqueous phosphate buffer (100 mM, pH 7.00) at an ionic strength of 0.50 M ($NaClO_4$), the Soret absorbance of AcMP8 varies linearly with concentration up to $\sim 3 \times 10^{-5}$ M, whereafter the slope decreases (Figure 3).[46a] The limiting slope of Figure 3 is $(1.55 \pm 0.01) \times 10^5$ M^{-1} cm^{-1}, in agreement with that obtained for monomeric MP8 ($(1.57 \pm 0.01) \times 10^5$ M^{-1} cm^{-1}).[33] If it is assumed that the observed departure from linearity is the consequence of a simple dimerization equilibrium (eq 1, where M and D are monomeric and dimeric forms of

$$2M \overset{K_D}{\rightleftharpoons} D \qquad K_D = \frac{[D]}{[M]^2} \tag{1}$$

AcMP8, respectively), then the total absorbance A_T may be related to the absorbance in the absence of dimerization, A_M

(45) Ghinea, N.; Simionescu, N. *J. Cell Biol.* **1985**, *100*, 606.

(46) (a) Beer's law experiment: Successive dilutions of a solution of AcMP8, initially comprising 292 μL of a 9.25×10^{-5} M solution of the heme peptide and 208 μL of 100 mM pH 7.00 phosphate buffer ($\mu = 0.5$ M ($NaClO_4$)), were made in a 10 mm path length cuvette by adding known volumes of the diluent buffer solution. For the initial part of the study at high heme concentration, 250 μL aliquots were withdrawn after mixing and carefully injected into a 1 mm path length cuvette thermostated at 25 °C in the spectrometer turret. The solution was withdrawn after recording the absorbance at 397.2 nm and returned to the bulk solution prior to effecting the next dilution. Concentrations in the 17.7−54.0 μM range were covered using a 1 mm path length cuvette, before switching to 10, 20, 50, and 100 mm path length cells for measurements in the 9.14−11.8, 4.16−6.43, 1.72−2.72, and 0.846−1.25 μM concentration ranges, respectively. (b) Because the molar absorptivity of AcMP8 at 397.2 nm is large (1.55×10^5 M^{-1} cm^{-1}), small volumetric errors accompanying manipulation of the solutions, particularly during cuvette changeovers, tend to be amplified and are clearly evident in the absorbance data of Figure 3. Such errors are unavoidable in attempts to examine a wide heme concentration range to enable estimation of both the $\pi-\pi$ dimerization constant of the heme peptide and the molar absorptivity of the Soret band.

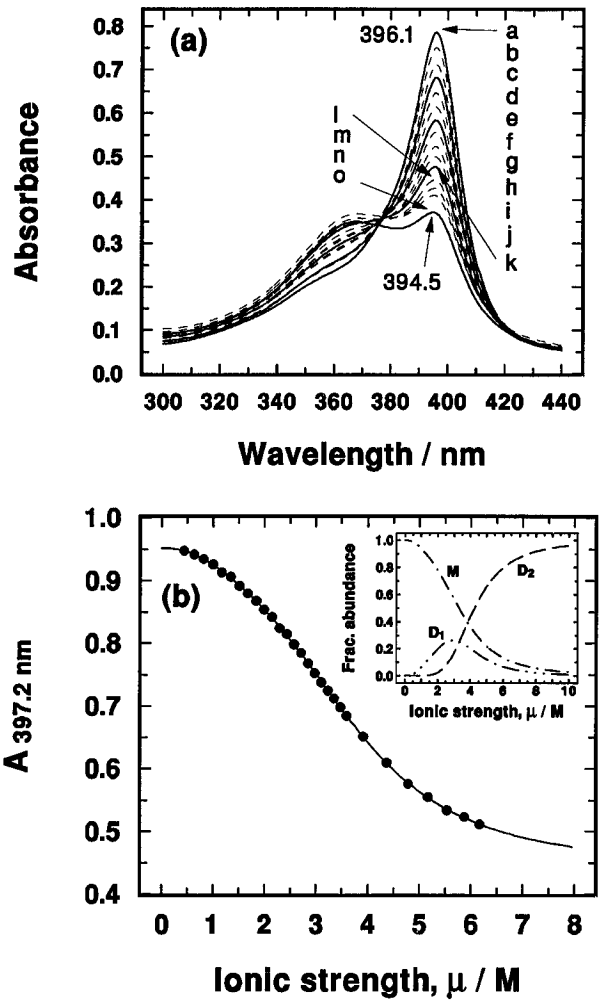

Figure 4. (a) Ionic strength dependence of the near-UV spectrum of AcMP8 (5.10 μM) at 25 °C (pH 7.00, 1.0 mM MOPS buffer). The total ionic strength (in M), 0.10, 0.50, 0.75, 1.00, 1.51, 1.76, 2.01, 2.26, 2.51, 2.76, 3.01, 3.26, 3.52, 3.77, and 4.02, from curves a to o, respectively, was adjusted using $NaClO_4$ as the noncoordinating salt. (b) Ionic strength dependence of the Soret band absorbance (397.2 nm, 20 mm path length cuvette) of an aqueous solution of AcMP8 (3.1 μM) at 25 °C and pH 7.0 (100 mM MOPS buffer). Both the absorbance and ionic strength data are corrected for dilution due to added $NaClO_4 \cdot H_2O$. The theoretical curve is a fit of the data to eq 5: $K_1 = (3.49 \pm 0.01) \times 10^{-2}$ M^{-3}, $m = 2.24 \pm 0.00_3$, $K_2 = (6.99 \pm 0.05) \times 10^{-3}$ M^{-4}, and $n = 4.13 \pm 0.01$. The inset shows the fractional distribution of the AcMP8 monomer (M), weakly packed dimer (D_1), and tightly packed dimer (D_2) as a function of ionic strength extrapolated to 10 M.

($=\epsilon_M C$), by eq 2, where ϵ_M and ϵ_D are the molar absorptivities

$$A_T = \epsilon_M C_0 - (2\epsilon_M - \epsilon_D)\left[\frac{4K_D C_0 + 1 - (1 + 8K_D C_0)^{1/2}}{8K_D}\right] \quad (2)$$

of the monomer and dimer, respectively, and C_0 is the total chromophore concentration.[8a] (The derivation of eq 2 is given in the Supporting Information.)

As seen in Figure 3, a rather poor fit of the data was obtained with eq 2; best estimates of K_D, ϵ_M, and ϵ_D were $(1.09 \pm 0.06) \times 10^4$ M^{-1}, $(1.88 \pm 0.02) \times 10^5$ M^{-1} cm^{-1}, and $(1.09 \pm 0.07) \times 10^5$ M^{-1} cm^{-1}, respectively. Systematic deviation of the fit at higher concentrations suggests that this model is valid only for [AcMP8] $\lesssim 40$ μM.

Ionic Strength Effects. The UV spectra of AcMP8 (Figure 4a) show that progressively increasing the ionic strength of an aqueous solution of the heme peptide (pH 7.00, 1.0 mM MOPS buffer, 25 °C) with $NaClO_4$ as the noncoordinating salt, while keeping the total number of chromophore units constant, results in hypochromism of the Soret band and a small blue shift ($\lambda_{max,0.10M} = 396.1$ nm, $\lambda_{max,4.0M} = 394.5$ nm) of the absorption maximum. This is accompanied by the appearance of a broad, moderately intense band at 368 nm, which overlaps the weak N band of the initial spectrum located at ~355 nm. Between $\mu = 0.10$ and 3.01 M there are well-defined isosbestic points at 377 and 420 nm, but these give way to a single isosbestic point at 367 nm as the ionic strength increases further to 4.02 M.

A reduction in the electrostatic repulsion between negatively charged metalloporphyrin monomers on the addition of a salt can be expected to occur due to binding of the added cations by anionic groups on the porphyrin; this will favor the formation of π-stacked dimers.[10b] We assume that at least two equilibria are involved in bringing about the spectroscopic changes of Figure 4a, eqs 3 and 4, where M refers to monomeric AcMP8

$$2M^{j-} + mL^+ \overset{K_1}{\rightleftharpoons} D_1^{m-2j} \qquad K_1 = \frac{[D_1^{m-2j}]}{[M^{j-}]^2[L^+]^m} \quad (3)$$

$$D_1^{m-2j} + nL^+ \overset{K_2}{\rightleftharpoons} D_2^{m+n-2j} \qquad K_2 = \frac{[D_2^{m+n-2j}]}{[D_1^{m-2j}][L^+]^n} \quad (4)$$

at pH 7, D_1 the first more weakly associated dimer produced on binding of m cations (L^+) by M, and D_2 a second, more tightly packed dimer resulting from the binding of a further n cations by D_1. The total absorbance, A_T, is given by eq 5; A_n

$$A_T = \sum_{n=1}^{3} A_n \alpha_n \quad (5)$$

is the absorbance of the nth species, and α_n the fraction of that species in solution. The fractions of the monomer, M^{j-}, weakly packed dimer, D^{m-2j}, and tightly packed dimer, D^{m+n-2j}, are given in eqs 6−8. The values obtained from fitting the data to

$$\alpha_{M^{j-}} = \frac{-1 + \{1 + 8K_1[L^+]^m(1 + K_2[L^+]^n)\}^{1/2}}{4K_1[L^+]^m(1 + K_2[L^+]^n)} \quad (6)$$

$$\alpha_{D_1^{m-2j}} = \frac{1 - \alpha_{M^{j-}}}{2(1 + K_2[L^+]^n)} \quad (7)$$

$$\alpha_{D_2^{m+n-2j}} = \frac{1 - \alpha_{M^{j-}} - 2\alpha_{D_1^{m-2j}}}{2} \quad (8)$$

eq 5 (Figure 4b) at 25 °C were $K_1 = (3.49 \pm 0.01) \times 10^{-2}$ M^{-3}, $m = 2.24 \pm 0.00_3$, $K_2 = (6.99 \pm 0.05) \times 10^{-3}$ M^{-4}, and $n = 4.13 \pm 0.01$. The inset to Figure 4b shows plots of eqs 6−8 as a function of ionic strength extrapolated to 10 M.

Spectroscopic pK_a's. The pH dependence of the electronic spectrum of AcMP8 in an aqueous multicomponent buffer ($\mu_i = 0.1$ M) at 25 °C (Figure 5) shows a red shift of the Soret (B) band ($\lambda_{max,pH1.4} = 393.8$ nm, $\lambda_{max,pH12.8} = 405.6$ nm) accompanied by a drop in the initial intensity to 52% at pH 10.5, followed by 7% hyperchromism in going from pH 10.5 to pH 12.8. These changes in the Soret band are consistent with a progressive transition from a predominantly high-spin ferric state to a predominantly low-spin ferric state at high pH.[13b] At low pH, the visible region bands at 495 nm (Q_v: a_{1u},$a_{2u}(\pi) \rightarrow e_g^*(\pi^*)$, (1,0) vibronic component of the Q−B coupled states), 530 nm (Q_o: a_{1u},$a_{2u}(\pi) \rightarrow e_g^*(\pi^*)$), 570 nm ($a_{2u}'(\pi) \rightarrow e_g(d\pi)$),[13d]

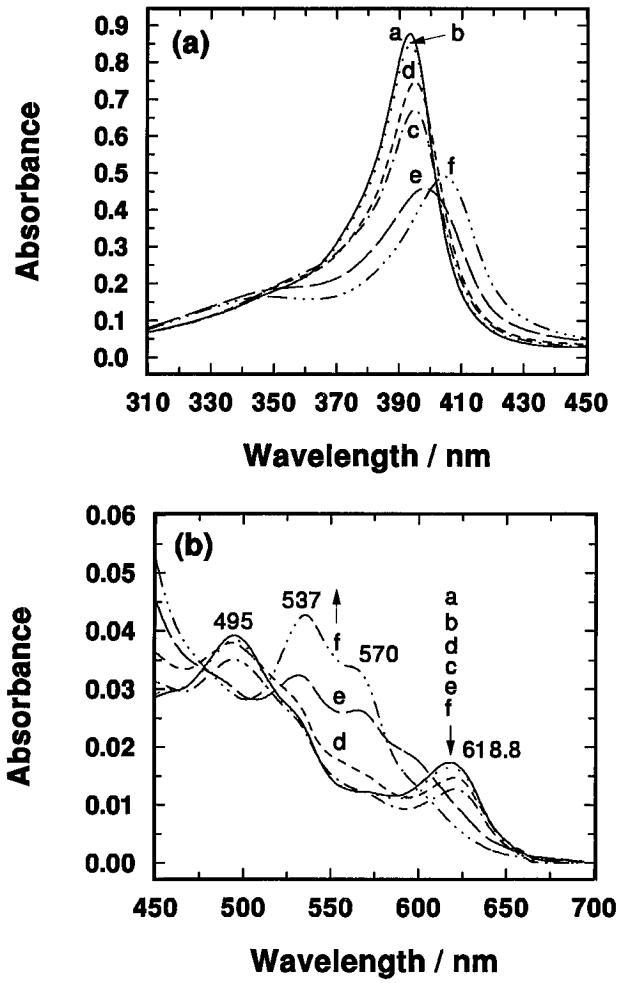

Figure 5. pH dependence of the near-UV (a) and visible-region (b) spectra of AcMP8 (5.09 μM, 10 mm path length cell) in an aqueous multicomponent buffer at 25 °C (0.10 M KCl and 1.0 mM each of potassium hydrogen phthalate, MES, MOPS, Tris, and CHES). pH values (Soret band maxima, nm): (a) 1.40 (393.8); (b) 2.50 (393.8); (c) 4.00 (395.0); (d) 7.00 (396.1); (e) 10.51 (399.1), and (f) 12.81 (405.6).

and 618.8 nm ($b_{2u}(\pi) \rightarrow e_g(d\pi)$)[13d] indicate that the Fe(III) ion in AcMP8 is in a predominantly $S = {}^5/_2$ state between pH 1.4 and 7.0. The assignments in parentheses are for a heme group with D_{4h} symmetry, in accord with the current convention.[13b] The $S = {}^5/_2$ CT band ($b_{2u}(\pi) \rightarrow e_g(d\pi)$) observed at ∼619 nm below pH 7.0 is displaced to ∼600 nm at pH 10.5; the shift to higher energy of the $d\pi$ orbitals of the sextet species is suggestive of a change in the axial ligands at the metal. The weaker $a_{2u}'(\pi) \rightarrow e_g(d\pi)$ CT band of the $S = {}^5/_2$ species, which is typically located 50 nm (∼1400 cm^{-1}) to the blue of the first CT band,[13b] is then not observable due to overlap with the more intense Q_o and Q_v bands of the $S = {}^1/_2$ state. The shoulder at ∼490 nm (pH 10.5) is probably the blue-shifted Q_o band of the sextet species, although it may be the vibronically allowed (3,0) component of the Q−B coupled states of the spin singlet.[13b] The pH 10.5 electronic spectrum of AcMP8 is therefore consistent with an equilibrium between $S = {}^1/_2$ and ${}^5/_2$ states. At pH 12.8, relatively little of the intensity at 490 and 600 nm remains and the Q_o (570 nm) and Q_v (537 nm) bands of the low-spin ($S = {}^1/_2$) state dominate the visible spectrum.

There is an interesting, well-resolved spectroscopic transition attending the change in pH from 2.50 to 7.00 in the Soret region. Figure 5a shows that the intensity of the B band drops considerably (by ∼20%) between pH 2.50 (λ_{max} = 393.8 nm) and pH 4.00 (λ_{max} = 395.0 nm) before increasing by ∼10%

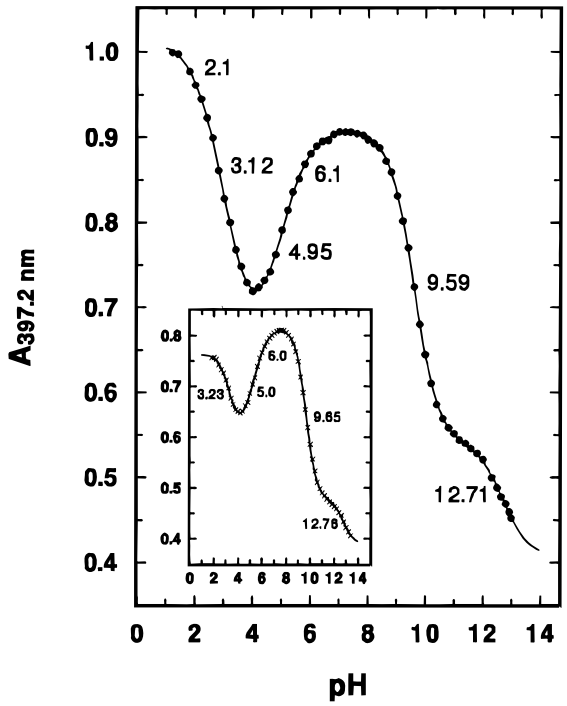

Figure 6. Variation of the Soret absorbance (397.2 nm) with pH for the titration of 3.1 μM AcMP8 at 25 °C with NaOH (pH 6−13.5) and HCl (pH 8−1.6), in aqueous buffered solution ($\mu \approx 0.1$ M) and in a 20 mm path length cuvette. The theoretical curve (eq 9) was fitted to the data over the full pH range and is consistent with six overlapping pK_as: pK_1 = 2.1 ± 0.2, pK_2 = 3.12 ± 0.07, pK_3 = 4.95 ± 0.07, pK_4 = 6.1 ± 0.3, pK_5 = 9.59 ± 0.01, pK_6 = 12.71 ± 0.05. The inset shows the analogous data at 25 °C for the *c*-terminal *n*-propylamide derivative of AcMP8 (∼2.6 μM); the data are fitted to eq 9 for five pK_as (3.23 ± 0.04, 5.0 ± 0.1, 6.0 ± 0.2, 9.65 ± 0.01, 12.76 ± 0.06).

between pH 4.00 and pH 7.00 (λ_{max} = 396.1 nm). There are similar variations of intensity in the visible region (Figure 5b). The observed hypochromism of the B band from pH 2.50 to pH 4.00 does *not* reflect aggregation of the chromophore at its isoelectric point since (i) concurrent hyperchromism of the absorption envelope in the N band region is not observed and (ii) λ_{max} is displaced to *longer* wavelength rather than to shorter wavelength, as is common in aggregated systems (Figure 4a).[22] The spectroscopic changes between pH 4.00 and pH 7.00 are, for similar reasons, inconsistent with those attending aggregation of the chromophore.

Figure 6 shows the change in absorbance at 397.2 nm as a function of pH for an aqueous solution of AcMP8 at 25 °C (μ = 0.10 M, $NaClO_4$). The experimental data were fitted to an ionization isotherm (eq 9) describing six consecutive equilibria,

$$A_T = \sum_{n=1}^{7} A_n \alpha_n \tag{9}$$

where A_T is the total solution absorbance, A_n the absorbance of the *n*th species, and α_n the fraction of that absorbing species in solution. The last is given by eq 10, where K_i is the *i*th

$$\alpha_n = \frac{[H^+]^{7-n}\prod_{i=1}^{n-1} K_i}{\sum_{j=0}^{6}([H^+]^j \prod_{i=1}^{6-j} K_i)} \tag{10}$$

ionization constant. The values of the six spectroscopic pK_a's obtained from the theoretical curve fitting the data (Figure 6)

were $pK_1 = 2.1 \pm 0.2$, $pK_2 = 3.12 \pm 0.07$, $pK_3 = 4.95 \pm 0.07$, $pK_4 = 6.1 \pm 0.3$, $pK_5 = 9.59 \pm 0.01$, and $pK_6 = 12.71 \pm 0.05$ (rmsd $= 2.00 \times 10^{-3}$). Analogous equations with five or four pK_a's (Figures S1−S3, Supporting Information) gave significantly poorer fits. The inset to Figure 6 shows the variation in absorbance (397.2 nm) with pH for an aqueous solution of the first HPLC-purified reaction product of AcMP8 with *n*-propylamine/EDC at 25 °C ($\mu_i = 0.10$ M, KCl). The data are fitted to eq 9 for five pK_a's (3.23 ± 0.04, 5.0 ± 0.1, 6.0 ± 0.2, 9.65 ± 0.01, and 12.76 ± 0.06; rmsd $= 2.71 \times 10^{-3}$). Parts a−e of Figure S3 indicate that for both AcMP8 and the first of its *n*-propylamine/EDC reaction products, an acceptable random distribution of fit residuals is obtained only when *two* pK_a's are fitted to the spectroscopic data between pH 4 and 7—a single pK_a in this pH range provides a statistically inadequate fit of the data. Importantly, the spectroscopic titration data for the *n*-propylamide derivative of AcMP8 (inset to Figure 6) clearly demonstrate (i) the absence of the first pK_a shown by AcMP8 and (ii) a pH-dependent behavior nearly identical to that of AcMP8 over the remainder of the full pH range.

The temperature dependence of the pK_a fitting the optical transition between pH 7.5 and pH 10.8 (Figure 6) was examined between 5 and 35 °C and conforms to a linear van't Hoff isochore (Figure S4, correlation coefficient $= -0.9996$). This pK_a (pK_{H_2O}) is attributed to the ionization of coordinated water *trans* to His-18 (eq 11), for which $\Delta H = 48 \pm 1$ kJ mol^{-1} and $\Delta S = -22 \pm 3$ J K^{-1} mol^{-1} at 25 °C and $\mu = 0.10$ M.

$$\mathrm{HHis{-}Fe^{3+}{-}OH_2} \underset{}{\overset{K_{H_2O}}{\rightleftharpoons}} \mathrm{HHis{-}Fe^{3+}{-}OH^-} + \mathrm{H^+} \qquad (11)$$

Plots of ln K against $1/T$ for the other spectroscopic pK_a's of AcMP8 were not linear. In the pH <4 range, pK_1 and pK_2 were highly correlated at all temperatures, indicating considerable overlap of the two equilibria. Furthermore, although single pK_a's could be fitted to the data in the pH ranges 1−4 and 4−7, they failed to yield linear van't Hoff relationships. Comparison of the two curves shown in Figure 6 strongly suggests that more than one ionization equilibrium contributes to the optical transition of AcMP8 below pH 4, while more than one ionization appears to be optically active between pH 4 and 7 in both AcMP8 and the first of its reaction products with *n*-propylamine/EDC. The existence of overlapping equilibria throughout the low-pH range clearly limits the possibility of obtaining linear van't Hoff relationships for the fitted pK_a's.

At pH >13.0, there are slow time-dependent changes in the spectrum of AcMP8. Their kinetics were monitored at pH 13 ($[Fe]_0 = 5.73$ μM) and pH 14 ($[Fe]_0 = 5.73$ and 11.75 μM) at 25 °C. An examination of the initial rates showed that the process is second-order in [Fe] and zero-order in [OH$^-$], and the absorbance−time traces could be fitted by an equation appropriate for a process[47] second-order in chromophore (Figure S5, Supporting Information), affording a mean rate constant of 2.59 ± 0.14 M^{-1} s^{-1}. The time-dependent changes in the electronic spectrum of AcMP8 (11.75 μM, 25 °C) at pH 14.0 in both the UV and visible regions (Figure S6a−e, Supporting Information) are consistent with two main processes: (i) a change in spin state from predominantly $S = {}^1/_2$ to $S = {}^5/_2$ Fe(III) and (ii) aggregation of the chromophore. Reflecting the change in spin state with time, the low-spin bands[13b] at 537.0 nm (Q_v) and 564.9 nm (Q_o) diminish in intensity while a shoulder initially at 608.5 nm generates the characteristic CT band at 601.7 nm of an $S = {}^5/_2$ ferric porphyrin complex axially ligated by an anionic oxygen ligand,[13b] which becomes the dominant spectroscopic feature in the visible spectrum after ~100 h. There is also a concurrent shift in the B band from 407.0 to 394.8 nm as the low-spin starting material is consumed. Aggregation becomes more pronounced at $t > 60$ h and, in its final stages, is earmarked by distinct hypochromism of the B band, accompanied by hyperchromism of the spectrum in the N band region, which is characteristic of heme aggregates.[7a]

(47) Laidler, K. J. *Chemical Kinetics*, 3rd ed.; Harper & Row: New York, 1987; p 22.

Discussion

Preparation of AcMP8. Yang and Sauer[37] apparently published the first report on AcMP8, but no conditions for the preparation of the protected heme octapeptide were given. Wang and Van Wart[40] reported a procedure for the acetylation of MP8 using a 500 molar excess of acetic anhydride at room temperature. In our experience, MP8 and AcMP8 coelute on RP HPLC under the conditions they employed.[40] The HPLC procedure reported here clearly separates the two (Figure 2) and shows that there is essentially complete conversion of MP8 to AcMP8.

Monomeric AcMP8. Protection of the α-NH_2 group of Cys-14 significantly decreases the deviation of the chromophore from Beer's law (Figure 3), even at an ionic strength of 0.5 M. We found no spectroscopic evidence for concentration-dependent formation of low-spin AcMP8 at higher heme concentrations, the spectra (not shown) suggesting that a change in the state of axial ligation of AcMP8 does not attend its aggregation. By eliminating the possibility of intermolecular coordination *via* pendant ligating residues of the polypeptide chain, aggregation is restricted to $\pi-\pi$ interactions between heme groups; K_D for AcMP8 ($(1.09 \pm 0.06) \times 10^4$ M^{-1}) is therefore an order of magnitude lower than that for MP8 ($(1.17 \pm 0.02) \times 10^5$ M^{-1}; $\mu = 0.1$ M, pH 7.00, 25 °C).[33] The simple dimerization model (eq 2) applies only to the lower concentration range of the study. At higher chromophore concentrations, both MP8[33] and AcMP8 (Figure 3)[46b] exhibit significant departures from the theoretical curve, suggesting, in agreement with the results of Urry and Pettegrew,[22] that formation of higher aggregates ensues. Protection of the α-NH_2 group of Cys-14 allows for concentrations up to $\sim 3 \times 10^{-5}$ M AcMP8 to be studied in aqueous solution ($\mu = 0.5$ M).

Ionic Strength Effects. Shelnutt and co-workers[10b] have shown that some metallouroporphyrins dimerize in the presence of added NaCl or LiCl according to a simple monomer−dimer equilibrium. Their model treats the equilibrium in terms of diminished electrostatic repulsion between monomers as a result of charge neutralization by the added cations. White and Plane[7b] found that dimerization of tetraalkylammonium porphyrins carrying a total charge of +4 at pH 5 depended on the identity of the electrolyte anion and on the length of the peripheral alkylamine substituent chains, with the stability constants decreasing with increasing chain length.

Figure 4a indicates that the electronic spectrum of AcMP8 is strongly dependent on ionic strength. The isosbestic points initially at 377 and 420 nm (0.10 M $< \mu <$ 3.01 M) are replaced by at least one isosbestic point at 367 nm ($\mu >$ 3.01 M), suggesting that the initial equilibrium gives way to a second at higher ionic strength. It is assumed that, in the first equilibrium (eq 3), AcMP8 monomers, carrying a total molecular charge of $j-$ at pH 7.0, dimerize due to reduced electrostatic repulsion brought about by specific binding of m Na^+ ions (L^+). If $(m - 2j) \neq 0$, the dimer carries a residual negative charge which permits only weak face-to-face π-stacking of the monomer units. Increasing the ionic strength drives the second equilibrium (eq 4) in which all or virtually all anionic sites on the weakly packed

dimer are neutralized so that a more tightly packed dimer of total charge $(m + n - 2j) \approx 0$ is produced. Figure 4b shows that this model fits the experimental data very well. Importantly, the refined parameters from eq 5 for m and n (2.24 and 4.13, respectively) indicate that the charge on the AcMP8 monomer at pH 7.0 is *ca.* 3−; i.e., $j = 3$. It will be shown (*vide infra*) that this result has a pivotal bearing on complete assignment of the pH-dependent forms of AcMP8 from the spectroscopic titration data.

If eq 3 is rewritten as eqs 12 and 13 and eq 4 as eq 14, then eq 15 follows where the fractions of the absorbing species are given in eqs 16−19.

$$M^{j-} + aL^{+} \overset{K'_1}{\rightleftharpoons} M^{a-j} \qquad K'_1 = \frac{[M^{a-j}]}{[M^{j-}][L^{+}]^a} \tag{12}$$

$$2M^{a-j} \overset{K'_2}{\rightleftharpoons} D_1^{\,2(a-j)} \qquad K'_2 = \frac{[D_1^{\,2(a-j)}]}{[M^{a-j}]^2} \tag{13}$$

$$D_1^{\,2(a-j)} + bL^{+} \overset{K'_3}{\rightleftharpoons} D_2^{\,b+2a-2j} \qquad K'_3 = \frac{[D_2^{\,b+2a-2j}]}{[D_1^{\,2(a-j)}][L^{+}]^b} \tag{14}$$

$$A_T = \sum_{n=1}^{4} A_n \alpha_n \tag{15}$$

$$\alpha_{M^{j-}} = \{-(1 + K'_1[L^{+}]^a) + \{(1 + K'_1[L^{+}]^a)^2 + 8K'_1{}^2K'_2[L^{+}]^{2a}(K'_3[L^{+}]^b + 1)\}^{1/2}\}/ 4K'_1{}^2K'_2[L^{+}]^{2a}(K'_3[L^{+}]^b + 1) \tag{16}$$

$$\alpha_{M^{a-j}} = \{-(1 + K'_1[L^{+}]^a) + \{(1 + K'_1[L^{+}]^a)^2 + 8K'_1{}^2K'_2[L^{+}]^{2a}(K'_3[L^{+}]^b + 1)\}^{1/2}\}/ 4K'_1K'_2[L^{+}]^{a}(K'_3[L^{+}]^b + 1) \tag{17}$$

$$\alpha_{D_1^{\,2(a-j)}} = \frac{1 - \alpha_{M^{j-}} - \alpha_{M^{a-j}}}{2(K'_3[L^{+}]^b + 1)} \tag{18}$$

$$\alpha_{D_2^{\,b+2a-2j}} = \frac{1 - \alpha_{M^{j-}} - \alpha_{M^{a-j}} - 2\alpha_{D_1^{\,2(a-j)}}}{2} \tag{19}$$

Of the nine parameters to be fitted in eq 15, five are identical to those of the simpler isotherm (eq 5); these were fixed for the nonlinear curve-fitting procedure. The three parameters K'_1, a, and K'_2 of eqs 12 and 13 obtained from fitting eq 15 to the data in Figure 4b were $(1.47 \pm 0.00_3) \times 10^{-3}$ M^{-1}, $1.12 \pm 0.00_2$, and $(1.60 \pm 0.01) \times 10^4$ M^{-1}, respectively. The value of a is exactly half the value of m in eq 5, which indicates that a reliable fit of the extended model to the data in Figure 4b may be obtained by this procedure. The self-association stability constant ($\log K'_2 = 4.20 \pm 0.00_2$) is in agreement with that obtained from the Beer's law study of AcMP8 at pH 7.0 (Figure 3, $\log K_D = 4.04$) and is consistent with the data for metallouroporphyrins reported by Shelnutt and co-workers,[10b] who found that the log of the stability constant ranged from 3.0 in [VO(UroP)] to 4.8 in [Pt(UroP)]. Moreover, the dimerization constant for AcMP8 at pH 7 is similar to the values found by White and Plane[7b] for metal-free tetraalkylammonium porphyrins (pH 5) at low ionic strength, suggesting that $\log K_D \sim 4$ reflects the intrinsic propensity of porphyrin and metalloporphyrin π-systems to associate in aqueous solution. Possible structures for the two salt-stabilized AcMP8 dimers, D_1 and D_2, are considered in detail in part 2.[41a]

Spectroscopic pK_a's of AcMP8: The Acid Range. Figure 6 shows that there are at least six pK_a's observable in the electronic spectrum of AcMP8. Their interpretation is summarized in Scheme 1. At pH <1.5, we propose that AcMP8 exists as the six-coordinate $S = {}^5/_2$ diaqua complex and that the first transition ($pK_1 = 2.1 \pm 0.2$) involves coordination of the *c*-terminal carboxylate group (Glu-21) of the appended polypeptide chain.[48] The electronic spectrum (envelope a in Figure 5) at pH 1.40 is consistent with a pure high-spin state; the energy and molar absorptivity of the B band ($\epsilon_{393.8nm} = 1.76 \times 10^5$ M^{-1} cm^{-1}) reflect axial ligation by two weak-field ligands, while the visible bands Q_v (495 nm), Q_o (530 nm), $a_{2u}'(\pi) \rightarrow e_g(d\pi)$ (570 nm), and $b_{2u}(\pi) \rightarrow e_g(d\pi)$ (620 nm) are distinctly those resulting from a $(t_{2g})^3(e_g)^2$ configuration of the metal.[13d] The spectrum at pH 2.50 (envelope b in Figure 5) shows that the B, Q_v, and Q_o bands decrease slightly in intensity, but without a shift in energy. The $S = {}^5/_2$ configuration at the metal is therefore retained in this equilibrium, although the decrease in intensity of the B band suggests that the axial ligand field strength at the metal is somewhat enhanced. This is expected when exchanging a weak-field neutral oxygen donor ligand (H_2O) for a weak-field anionic oxygen donor such as a carboxylate group ($RCOO^-$).

The proposed change in axial ligation of AcMP8 below pH 3 is supported by the spectroscopic titration of the first product of the reaction of AcMP8 with *n*-propylamine and EDC shown in the inset to Figure 6. The reaction between EDC and AcMP8 in the presence of *n*-propylamine results in stepwise conversion of each carboxylate group to the corresponding *n*-propylamide analog;[49a] protection of the carboxylate group with the lowest pK_a appears to occur first. Complete elimination of the low-pH transition of AcMP8 from the full pH profile upon protection of the *c*-terminal carboxylate group therefore suggests that the *c*-terminal carboxylate group of Glu-21 binds to the metal at low pH. Possible coordination of carboxylate groups in heme peptides has in fact been suggested for acetylated MP11,[24] although without convincing evidence, while Zewert *et al.*[49c] recently used NMR and EPR methods to show that the distal carboxylate group of a Val68Glu metMb mutant is coordinated at pH 7.

The second acid range transition for AcMP8 (Figure 6 and Scheme 1, $pK_a = 3.12 \pm 0.07$) probably involves deprotonation of cationic His-18 and concomitant replacement of the *c*-terminal carboxylate group by the neutral heterocyclic base. The electronic spectrum at pH 4.00 (envelope c in Figure 5) shows a significant intensity loss for the B band ($\epsilon_{395.0nm,pH4} = 1.35 \times 10^5$ M^{-1} cm^{-1}) and an accompanying red shift in the band maximum to 395.0 nm, consistent with coordination by a stronger field axial ligand; however, no major change in spin state occurs during this equilibrium (cf. visible-range spectrum). The Q_v band (495 nm) exhibits a lower intensity at pH 4.00 ($\epsilon_{495.0nm,pH4} = 6.82 \times 10^3$ M^{-1} cm^{-1}) relative to that at pH 2.50 ($\epsilon_{495.0nm,pH2.5} = 7.42 \times 10^3$ M^{-1} cm^{-1}), while the $S = {}^5/_2$ CT band at ~620 nm ($b_{2u}(\pi) \rightarrow e_g(d\pi)$) loses intensity ($\epsilon_{621.4nm,pH4}$

(48) (a) The pK_a of the *c*-terminal carboxylic acid group in proteins is 2.13.[48b] In the present case, interaction with the Fe(III) heme center (carrying a residual charge of +1) apparently does not significantly depress this pK_a. (b) *Handbook of Chemistry and Physics*, 55th ed.; Weast, R. C., Ed.; Chemical Rubber Co.: Cleveland, OH, 1974; pp D126−129.

(49) (a) Although we were able to easily isolate and spectroscopically characterize the first two reaction products, an EDC rearrangement product[49b] competes successfully with the coupling reaction and thus hampers isolation and characterization of the higher *n*-propylamide derivatives of the heme peptide. (b) Jones, J. H. *Amino Acid and Peptide Synthesis*; Oxford University Press: Oxford, U.K., 1992; pp 32−33. (c) Zewert, T. E.; Gray, H. B.; Bertini, I. *J. Am. Chem. Soc.* **1994**, *116*, 1169.

Scheme 1. Species Distribution as a Function of pH at 25 °C for AcMP8 in an Aqueous Multicomponent Buffer System[a]

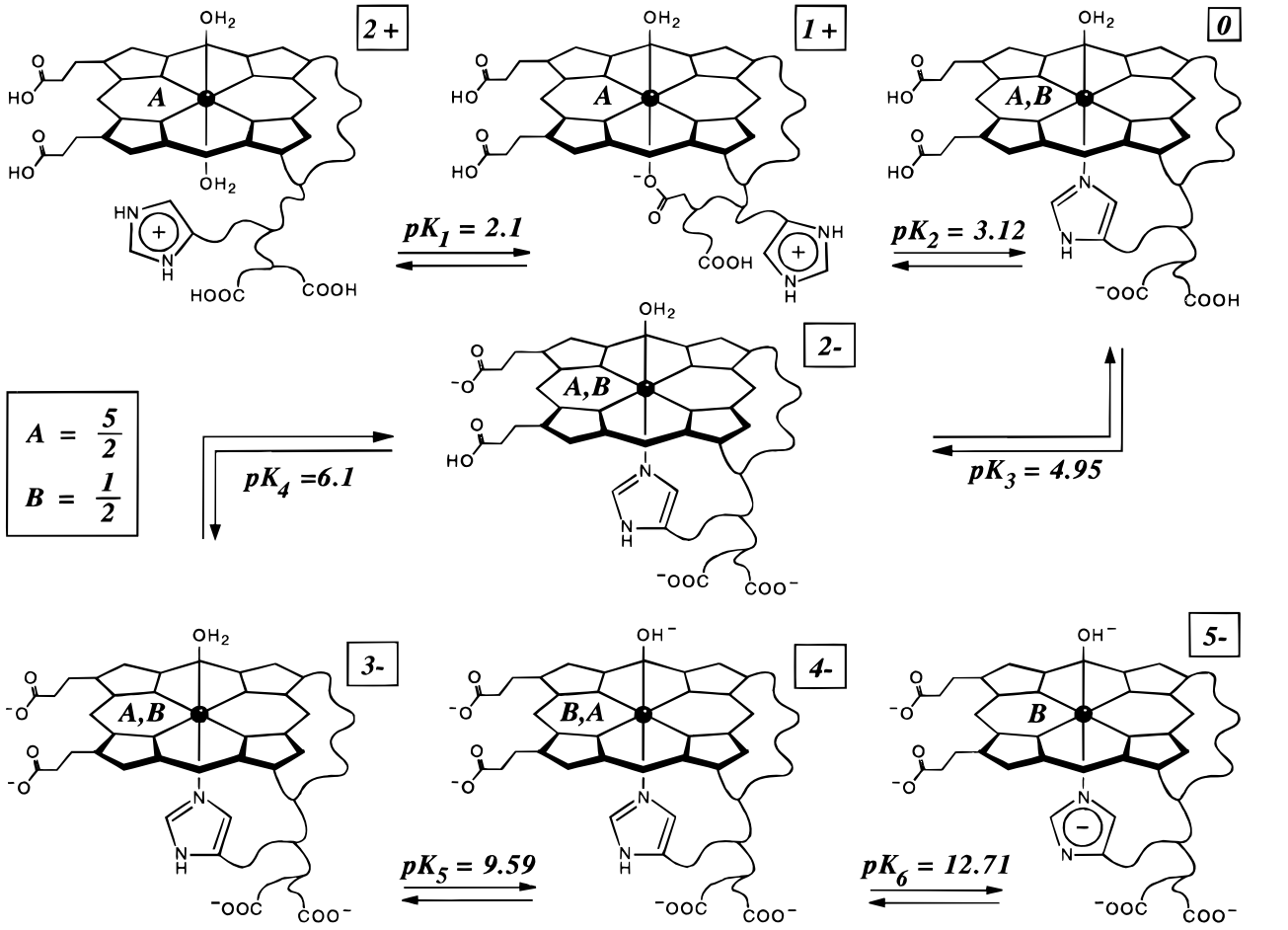

[a] The pK_a's are those determined by fitting eq 9 to the data in Figure 6, while structural assignments are based on the electronic spectra in Figure 5. The molecular charges are formal charges based on the number of cationic and anionic sites in each species. The dominant Fe(III) spin state (*A* or *B*) of each species at 25 °C is the first where two are indicated.

$= 2.51 \times 10^3$ M^{-1} cm^{-1} from $\epsilon_{618.8nm,pH2.5} = 3.06 \times 10^3$ M^{-1} cm^{-1}) and shifts by 2.6 nm to the red with the increase in pH from 2.50 to 4.00. The red shift of the CT band indicates that the dπ orbitals of the ferric ion are stabilized by coordination of the stronger σ-donor (histidine). (In low-spin complexes, this CT band occurs in the near-IR at ~1000 nm.[13d,50]) AcMP8 is therefore six-coordinate at pH 4.00, with H_2O *trans* to His-18, and remains predominantly in the $S = {}^5/_2$ state. High-spin five-coordinate heme proteins have broad Soret bands (width at half-height, $w_{1/2} = 50-60$ nm) of diminished intensity ($\epsilon \sim 1.0 \times 10^5$ M^{-1} cm^{-1}) relative to six-coordinate high-spin analogs, which have narrower ($w_{1/2} \sim 20-30$ nm), more intense B bands ($\epsilon \sim (1.6-1.8) \times 10^5$ M^{-1} cm^{-1}).[33] The spectroscopic data for AcMP8 at pH 4.00 are therefore consistent with an $S = {}^5/_2$ six-coordinate complex ($w_{1/2} = 29$ nm; $\epsilon_{max} = 1.35 \times 10^5$ M^{-1} cm^{-1}).[51] The present proposal that the pK_a at 3.12 reflects coordination of His-18 is consistent with ^{1}H NMR and other studies on several of the cytochromes *c*,[52−58] as well as studies on model heme peptides.[19] Reduction of the intrinsic value of pK_1 for histidine from ~6.00[59] in the free ligand to ~3 in coordinated histidine indicates that there is considerable competition between the metal ion and protons in solution for N(3) of the histidine residue.[60a]

The two pH-dependent optical transitions of AcMP8 in the pH range 4.0−7.6 (p$K_3 = 4.95 \pm 0.07$, and p$K_4 = 6.1 \pm 0.3$) are perhaps the most enigmatic of the four acid-range pK_a's (Figure 6). Although the data are fitted with two overlapping pK_a's in this range, the transition may be fitted, at the expense of an increased total rmsd, with a single pK_a of 5.08 ± 0.02 (Figures S1−S3). Given the fact that two pK_a's occur below pH 4, three pK_a's are the *minimum* number required to fit the acid-range data. However, a nonrandom distribution of residuals is observed (Figure S3) when a single pK_a is used to fit the titration data between pH 4 and 7, suggesting the likelihood of an additional pK_a in this region. The electronic spectrum at

(50) Thomson, A. J.; Gadsby, P. M. A. *J. Chem. Soc., Dalton Trans.* **1990**, 1921.
(51) However, since the Soret band molar absorptivity at pH 4.00 lies between the usual values for five- and six-coordinate complexes, the metal may be significantly displaced from the mean plane of the four porphinato nitrogens toward the proximal His-18 ligand; this would lead to a weaker Fe−O bond to water.
(52) Cohen, J. S.; Hayes, M. B. *J. Biol. Chem.* **1974**, *249*, 5472.
(53) Cohen, J. S.; Fisher, W. R.; Schechter, A. N. *J. Biol. Chem.* **1974**, *249*, 1113.
(54) Moore, G. R.; Williams, R. J. P. *Eur. J. Biochem.* **1980**, *103*, 513.
(55) Moore, G. R.; Williams, R. J. P. *Eur. J. Biochem.* **1980**, *103*, 523.
(56) Moore, G. R.; Pettigrew, G. W.; Pitt, R. C.; Williams, R. J. P. *Biochim. Biophys. Acta* **1980**, *590*, 261.
(57) Boeri, E.; Ehrenberg, A.; Paul, K. G.; Theorell, H. *Biochim. Biophys. Acta* **1953**, *12*, 273.
(58) Babul, J.; Stellwagen, E. *Biochemistry* **1972**, *11*, 1195.
(59) *Practical Handbook of Biochemistry and Molecular Biology*; Fasman, G. D., Ed.; CRC Press: Boca Raton, FL, 1989; p 34.
(60) (a) It may be noted that a synthetic iron(II) porphyrin coordinated by a single imidazole ligand in aqueous solution afforded a pK_a value of 3.6 for this equilibrium,[60b] demonstrating the effect that the decrease in positive charge on the metal ion has on this process. (b) Cannon, J.; Geibel, J.; Whipple, M.; Traylor, T. G. *J. Am. Chem. Soc.* **1976**, *98*, 3395.

pH 7.00 (envelope d in Figure 5) indicates that general hyperchromism of the visible and near-UV bands accompanies the shift in pH from 4.00 to 7.00. Moreover, while the energies of the visible bands remain practically unchanged, the B band exhibits a small red shift of 1.1 nm to 396.1 nm at pH 7.00. Since the $S = {}^5/_2$ configuration of the metal is preserved in this equilibrium (there are no changes in the $S = {}^5/_2$ visible bands) and all the main transitions constituting the absorption envelope appear to exhibit a uniform gain in oscillator strength, it seems unlikely that this pH-dependent transition demarcates a change in axial ligation of the metal. It is vital to establish the axial ligand combination for AcMP8 between pH 4 and 7, especially since a recent resonance Raman study on ferric *Aplysia* metMb has shown that the $S = {}^1/_2 \rightleftarrows S = {}^5/_2$ six-coordinate heme protein at pH 9.0 (HHis−Fe^{3+}(PPIX)−OH^-) loses water upon protonation (pK_a = 7.5) to form the corresponding high-spin five-coordinate complex (HHis−Fe^{3+}(PPIX)) at pH 6.0.[61] Moreover, whereas the high-spin five-coordinate geometry is preserved down to pH 4.0 in *Aplysia* metMb, partial conversion to the five-coordinate complex in horse metMb appears only to commence between pH 6.0 and 4.0, presumably because of differences in the distal heme environments of these proteins.[61]

In Scheme 1 we have assigned pK_3 (4.95 ± 0.07) to ionization of one of the heme propanoic acid groups and have shown concurrent ionization of the remote Glu-21 γ-COOH side chain. This is an assumption based on the pK_a (4.31) for this group in the free amino acid,[62] but in view of the distance of this residue from the heme chromophore, it is likely that the ionization is optically inactive at 397.2 nm. The second heme propanoic acid group is assigned to the ionization with pK_4 = 6.1 ± 0.3. It is assumed that the pK_a for this substituent is raised relative to that of free propanoic acid (4.69 ± 0.03, 25 °C, 0.1 M)[62] because of electrostatic repulsion between its conjugate base and the first propanoate group. It is noteworthy that the *c*-terminal *n*-propylamide derivative of AcMP8 also manifests two heme propanoic acid pK_a's in this region. Indeed, many NMR and redox studies on a variety of hemoproteins have shown that the ionization of one heme propanoic acid group occurs in the pH range 4.5−7.2, while that of the second, also falling within this range, is less frequently observed.[63−70] It has even been suggested that ionization of the heme propanoic acid substituents will be undetectable by optical spectroscopy,[71] although Moore *et al.*[56] were able to observe ionization of one of the heme propanoic acid groups of Fe(II) *Ps. aeruginosa* cytochrome *c*-551 from changes in the visible spectrum.

The uncertainty concerning the axial ligands and ionizing groups of AcMP8 in the pH 4−7 range may be resolved by performing the titration in the presence of a ligand (L) which binds Fe(III) and whose pK_a is low enough that competition with H^+ is insignificant in this range. If the pH 4−7 optical transition is *not* eliminated in the AcMP8···L system, then the pK_a's in question are likely to be due to ionization of the heme propanoic acid groups and *not* to the dissociation of iron-bound water or histidine.

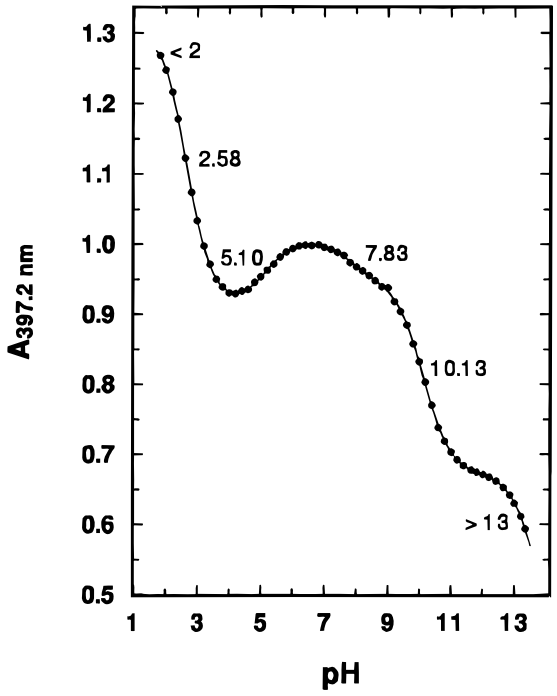

Figure 7. Plot of the Soret absorbance (397.2 nm) against pH for an aqueous buffered solution of AcMP8 (3.1 μM) containing 0.30 M 3-CNPy at a total initial ionic strength of 0.10 M (KCl). The spectroscopic titration was performed using concentrated NaOH and HCl in a 20 mm path length cuvette at 25 °C. The theoretical curve is a fit of the data to eq 9 for six consecutive ionizations with the following pK_as: pK'_1 < 2, pK'_2 = 2.58 ± 0.06, pK'_3 = 5.10 ± 0.03, pK'_4 = 7.83 ± 0.04, pK'_5 = 10.13 ± 0.01, pK'_6 > 13.

Figure 7 shows a fit (eq 9) of the pH dependence of the absorbance at 397.2 nm for a solution of AcMP8 in the presence of excess 3-CNPy; six consecutive ionization equilibria are evident. Figure 8 shows the near-UV and visible electronic spectra of the system at selected pH values. The pK_a of 3-CNPy is 1.64 (25 °C, μ = 0.1 M),[72] while the pH-independent constant for coordination to AcMP8, log *K*, is estimated to be ∼2.[73] The ligand therefore remains coordinated to the heme peptide in the pH range of interest (4.0−7.0) and *militates against possible aggregation near the pI value (*∼4), particularly at low concentration.

The values of the six spectroscopic pK_a's fitting the data for the AcMP8/3-CNPy system (Figure 7) were pK'_1 < 2.0, pK'_2 = 2.58 ± 0.06, pK'_3 = 5.10 ± 0.03, pK'_4 = 7.83 ± 0.04, pK'_5 = 10.13 ± 0.01, and pK'_6 > 13.0. The electronic spectra (Figure 8) indicate that AcMP8 exists as the $S = {}^5/_2$ diaqua complex at pH 1.70 but that a predominantly low-spin complex is formed at pH 4.20. The presence of the CT band ($b_{2u} \rightarrow e_g(d\pi)$) at 621 nm and the shoulder at 490 nm (Q_v band, $S = {}^5/_2$ complex), however, suggests that AcMP8···3-CNPy is an equilibrium mixture of $S = {}^1/_2$ and $S = {}^5/_2$ components, with an excess $S = {}^1/_2$ population at 25 °C. Spin equilibria of this sort have been observed for complexes of $[Fe(OEP)]^+$ with 3-ClPy.[74] The data indicate that the equilibrium for deproto-

(61) Rousseau, D. L.; Ching, Y.; Brunori, M.; Giacometti, G. M. *J. Biol. Chem.* **1989**, *264*, 7878.
(62) Smith, R. M.; Martell, A. E. *Critical Stability Constants*; Plenum Press: New York, 1989; Vol. 6, Second Supplement, p 302.
(63) Lommen, A.; Ratsma, A.; Bijlsma, N.; Canters, G. W.; Van Wielink, J. E.; Frank, J.; Van Beeumen, J. *Eur. J. Biochem.* **1990**, *192*, 653.
(64) Moore, G. R.; Pettigrew, G. W. *Cytochromes c. Evolutionary, Structural and Physicochemical Aspects*; Springer-Verlag: New York, 1990.
(65) Moore, G. R.; Williams, R. J. P.; Peterson, J.; Thomson, A. J.; Mathews, F. S. *Biochim. Biophys. Acta* **1985**, *829*, 83.
(66) La Mar, G. N.; Jackson, J. T.; Dugad, L. B.; Cusanovich, M. A.; Bartsch, R. G. *J. Biol. Chem.* **1990**, *265*, 16173 and the references therein.
(67) Costa, H. S.; Santos, H.; Turner, D. L.; Xavier, A. V. *Eur. J. Biochem.* **1992**, *208*, 427.
(68) Keller, R.; Groudinsky, O.; Wüthrich, K. *Biochim. Biophys. Acta* **1976**, *427*, 497.
(69) Goldsack, D. E.; Eberlein, W. S.; Alberty, R. A. *J. Biol. Chem.* **1966**, *241*, 2653.
(70) Marques, H. M. *Inorg. Chem.* **1990**, *29*, 1597.
(71) Barakat, R.; Strekas, T. C. *Biochim. Biophys. Acta* **1982**, *679*, 393.
(72) Martell, A. E.; Smith, R. M. *Critical Stability Constants*; Plenum Press: New York, 1982; Vol. 5, First Supplement, p 230.
(73) Munro, O. Q.; Marques, H. M. Unpublished work.

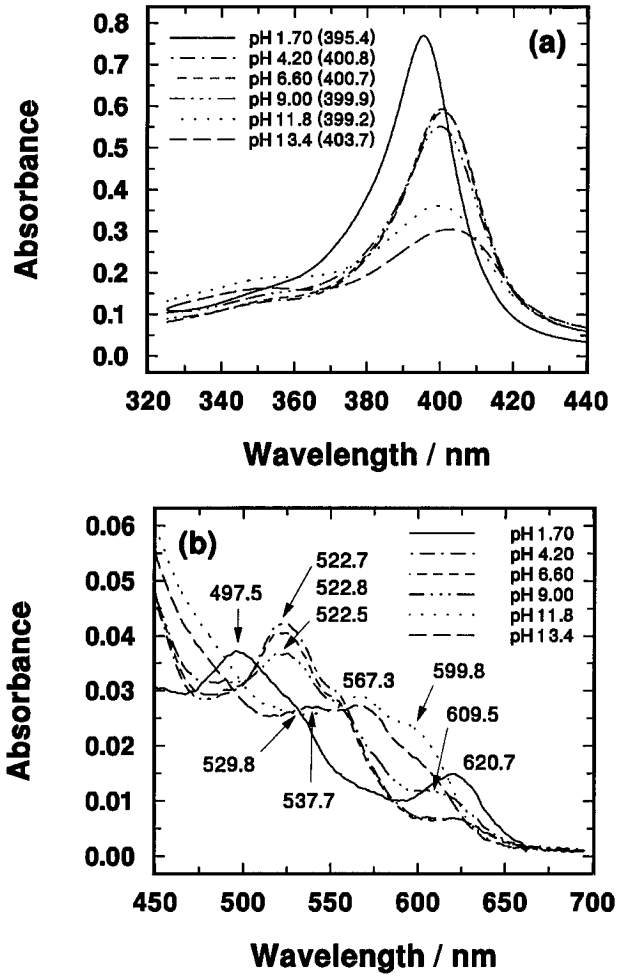

Figure 8. (a) pH dependence of the near-UV spectrum of AcMP8 (3.1 μM) in an aqueous buffered solution containing 0.30 M 3-CNPy. The spectra were recorded in 10 mm path length cuvettes at 25 °C at the indicated pH values. (b) Visible-range spectra for the AcMP8/3-CNPy system at discrete pH values between 1 and 14.

nation and coordination of His-18 ($pK'_2 = 2.58$) overlaps with that involving the binding of 3-CNPy ($pK'_1 < 2$). However, 3-CNPy cannot compete with His-18 for the proximal coordination site because (i) imidazoles bind more strongly than pyridines to microperoxidases,[19b] (ii) covalent attachment of His-18 to the heme group *via* the polypeptide chain greatly increases the local concentration of this ligand, and (iii) in all ligand binding work on AcMP8,[73] we have observed only one coordination equilibrium involving the metal ion, consistent with data for MP8[75] and MP6.[76] Interestingly, pK'_2 is lower in the 3-CNPy complex (2.60 ± 0.06) than in the aqua complex (3.12 ± 0.07), indicating that 3-CNPy binds to AcMP8 below pH 2 and is a powerful π-acceptor ligand capable of reducing electron density in the dπ orbitals.[77] (Stabilization of the six-coordinate HHis−Fe^{3+}−3-CNPy complex *via* π-bonding necessitates a higher $[H^+]$ to bring about decomplexation of His-18.) Axial ligation by 3-CNPy has further profound consequences in the alkaline range (*vide infra*).

Scheme 2 summarizes our interpretation of the pH-dependent transitions for the AcMP8/3-CNPy system. Coordination of 3-CNPy and the terminal carboxylate group (Glu-21) of AcMP8 brings about the first spectroscopic transition ($pK'_1 < 2.0$). Since coordination of two 3-CNPy ligands would produce mainly the low-spin complex, and the change in absorbance accompanying this equilibrium indicates that the $S = {}^5/_2$ state is maintained, two 3-CNPy ligands do not bind to the metal. From the data for AcMP8 in the absence of 3-CNPy (Figures 5 and 6), intramolecular coordination of the metal by the terminal carboxylate group of Glu-21 ($pK_a = 2.13$[48]) is highly probable. The resulting mixed-ligand system ($RCOO^-$−Fe^{3+}−3-CNPy), in which the carboxylate ligand competes successfully with 3-CNPy for one of the axial sites at the metal, will be high-spin since the axial ligand field is weaker than that produced by the ligand combination HHis−Fe^{3+}−OH_2 in AcMP8 at pH 7.0 (Scheme 1), which favors the S= ${}^5/_2$ state at 25 °C (*vide supra*). Deprotonation of cationic His-18 results in replacement of the weak-field carboxylate ligand ($pK'_2 = 2.60$) and triggers the spectroscopically observed switch in spin states between pH 2 and pH 4 (Scheme 2).

The spectroscopic titration in Figure 7 still shows the unique transition in the pH range 4.2−6.6 ($pK'_3 = 5.10 \pm 0.03$). However, since the spectra in Figure 8 indicate no change in spin state, we conclude that no change in the axial ligand combination (His-18, 3-CNPy) has occurred. The pK_a is in reasonable agreement with the mean ionization constant for the heme propanoic acid substituents of the HHis−Fe^{3+}−OH_2 complex (5.08 ± 0.02, Figure S2). The total change in absorbance at 397.2 nm accompanying this pH transition in AcMP8···3-CNPy is < 50% of that for AcMP8···OH_2, mainly because the former complex is predominantly low-spin and has a red-shifted B band ($\lambda_{max} = 400.7$ nm) relative to the high-spin aqua complex ($\lambda_{max} = 396.1$ nm). In Figure 8 it is evident that the intensity of the B band increases slightly at the expense of the Q_v band (Figure 8b) for the AcMP8···3-CNPy complex and, thus, on comparison with the data in Figure 5b, that the type of spectroscopic perturbation in the visible range brought about by ionization of the heme propanoic acid groups depends on the spin state of the metal. The third transition ($pK'_3 = 5.10$) in Scheme 2 is therefore depicted as involving ionization of the Glu-21 γ-carboxylic acid group (presumably spectroscopically silent at 397.2 nm) and the heme propanoic acid substituents; the latter perturb the electronic structure of the heme group and render the transition detectable.[78a] The alkaline transitions in the AcMP8/3-CNPy system are discussed later (*vide infra*).

Spectroscopic pK_a's of AcMP8: The Alkaline Range. Figure 6 indicates that there are two optical transitions above pH 7.5; the first ($pK_5 = 9.594 \pm 0.006$) corresponds to ionization of coordinated water, while we attribute the second

(74) Scheidt, W. R.; Geiger, D. K.; Haller, K. J. *J. Am. Chem. Soc.* **1982**, *104*, 495.
(75) Baldwin, D. A.; Marques, H. M.; Pratt, J. M. *J. Inorg. Biochem.* **1986**, *27*, 245.
(76) Saleem, M. M. M.; Wilson, M. T. *Inorg. Chim. Acta* **1988**, *153*, 93.
(77) (a) In the low-spin bis(cyanopyridine) complexes of $[Fe(TMP)]^+$ and $[Fe(TPP)]^+$, inversion of the ground state configuration from $(d_{xy})^2(d_{xz})^2(d_{yz})^1$ to mainly $(d_{xz},d_{yz})^4(d_{xy})^1$ is favored as a result of axial coordination of these powerful π-acceptor ligands and concomitant stabilization of the dπ orbitals.[77b,c] (b) Safo, M. K.; Gupta, G. P.; Watson, C. T.; Simonis, U.; Walker, F. A.; Scheidt, W. R. *J. Am. Chem. Soc.* **1992**, *114*, 7066. (c) Safo, M. K.; Walker, F. A.; Raitsimring, A. M.; Walters, W. P.; Dolata, D. P.; Debrunner, P. G.; Scheidt, W. R. *J. Am. Chem. Soc.* **1994**, *116*, 7760.
(78) (a) The present results for AcMP8 indicate that our previous interpretations of the acid-range data for MP8[75] and MP9[78b] in aqueous methanol solution are probably incorrect. We reported a single acid-range pK_a for MP8 of 4.43 ± 0.09.[75] However, re-evaluation of the data affords three pK_as which probably correspond to coordination of the *c*-terminal carboxylate (2.2), the binding of His-18 (3.5), and ionization of the heme propanoic acid substituents (4.9). Two pK_as were found for MP9: 2.9 ± 0.4 and 4.45 ± 0.05.[78b] It now appears likely that the first is due to coordination of His-18 while the second is probably a mean ionization constant for the two heme propanoic acid groups. (b) Baldwin, D. A.; Mabuya, M. B.; Marques, H. M. *S. Afr. J. Chem.* **1987**, *40*, 103.

Scheme 2. Species Distribution as a Function of pH at 25 °C for AcMP8 in an Aqueous Multicomponent Buffer System Containing 0.30 M 3-Cyanopyridine[a]

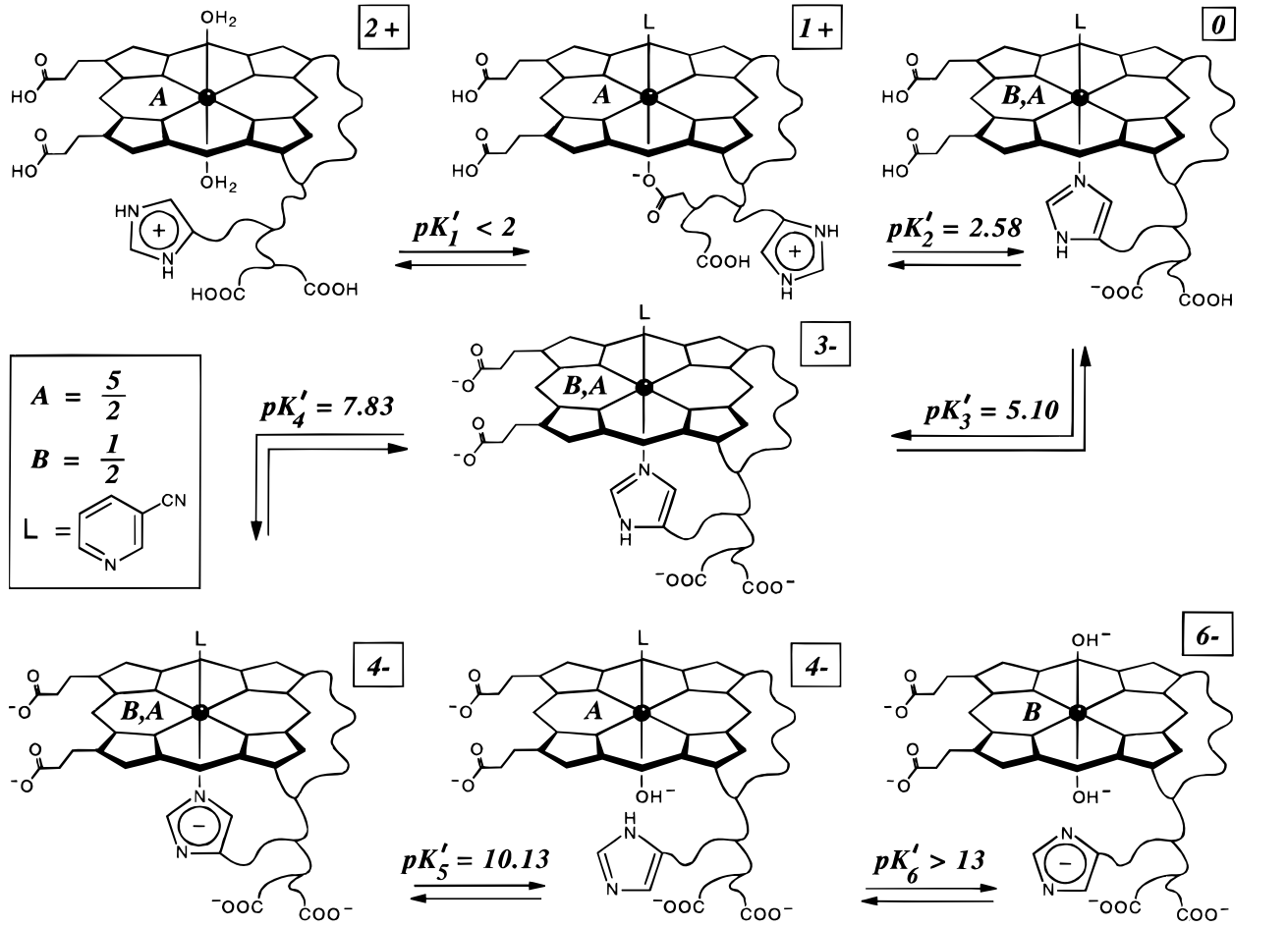

[a] pK_a's were determined by fitting eq 9 to the data in Figure 7, while structural assignments are based on the electronic spectra in Figure 8. Molecular charges were determined as in Scheme 1. The dominant Fe(III) spin state (*A* or *B*) of each species at 25 °C is the first where two are indicated.

Table 1. Selected Thermodynamic Data for the Ionization of Iron-Bound Water (pK_{H_2O}) in AcMP8 and Various Ferric Hemoproteins with the Axial Ligand Combination HHis−Fe^{3+}−OH_2[a]

ferrihemoprotein/model	pK_{H_2O}	ΔH/kJ mol^{-1}	ΔS/J K^{-1} mol^{-1}	ΔG/kJ mol^{-1}	T/°C	μ/M
cow Hb[b]	8.23 ± 0.02	6.57	−135	46.0	20	0.05
Aplysia Mb[c]	7.6 ± 0.1	14 ± 2	−98.49 ± 7.11	42.7 ± 0.4	20	0.20
Chironomus Hb[c]	7.48 ± 0.05	15 ± 1	−91.34 ± 4.31	41.8 ± 0.3	20	0.20
horse Hb[d]	8.86 ± 0.02	16.4 ± 2.1	−114 ± 7.5	49.8 ± 0.1	20	→0
baboon Hb[b]	8.11 ± 0.02	19.5	−88.7	45.6	20	0.05
hyena Hb[b]	8.30 ± 0.02	23.0	−80.3	46.4	20	0.05
horse Mb[e]	9.04 ± 0.03	24.1 ± 2.8	−90.8 ± 10	50.6 ± 0.2	20	→0
sperm whale Mb component IV[f]	8.93	24.6	−88.3	50.92	25	0.01
sperm whale Mb component IIIA[f]	9.03	28.8	−76.6	51.67	25	0.01
mouse Hb[b]	8.00 ± 0.02	29.9	−51.5	44.8	20	0.05
sperm whale Mb component II[f]	9.07	31.0	−69.9	51.9	25	0.01
pig Hb[b]	8.21 ± 0.02	32.9	−44.8	46.0	20	0.05
shrew Hb[b]	8.28 ± 0.02	42.7	−13	46.4	20	0.05
AcMP8[g]	9.59 ± 0.01	48.1 ± 0.8	−23 ± 3	54.81 ± 0.04	25	0.10

[a] The data are organized in the order of increasing ΔH. [b] Reference 79. [c] Reference 80. [d] Reference 81. [e] Reference 82. [f] Reference 83. [g] This work.

(pK_6 = 12.71 ± 0.05) to deprotonation of the proximal His-18 ligand to form the corresponding $S = {}^1/_2$ imidazol*ate* complex (Scheme 1).

Table 1 lists thermodynamic data for the aqua−hydroxo equilibrium of AcMP8 and representative heme proteins with analogous axial ligation. AcMP8 has the most positive ΔH and one of the most positive ΔS values in the series. Plots of ΔH against ΔS *at a fixed ionic strength* (0.05 M) are linear and reflect compensation of these two parameters to yield a value of ΔG for the different hemoglobins that varies by less than 10% for the species shown (mean $\Delta G = 47 \pm 3$ kJ mol^{-1}).[79−83] Taking cognizance of the differences in ionic strength, which have a significant effect on ΔH and ΔS,[79,84−86] the value of

(79) (a) Beetlestone, J. G.; Irvine, D. H. *J. Chem. Soc.* **1965**, 3271. (b) Beetlestone, J. G.; Irvine, D. H. *J. Chem. Soc.* **1964**, 5090.
(80) Brunori, M.; Amiconi, G.; Antonini, E.; Wyman, J.; Zito, R.; Fanelli, A. R. *Biochim. Biophys. Acta* **1968**, *154*, 315.
(81) George, P.; Hanania, G. I. H. *Biochem. J.* **1953**, *55*, 236.

ΔG for AcMP8, while different from the mean value for the hemoglobins, is similar to the values for the myoglobins (Table 1). The observed compensation of ΔH and ΔS is a property of water as the solvent,[87] but the value of ΔG depends on the coordination sphere environment of the metal ion.[88] In the present case, ΔG varies by only 13 kJ mol^{-1} (Hbs, Mbs, and AcMP8) and is a signature of the similar ligation state (HHis, H_2O) of the Fe(III) ion in these hemoproteins and the model system.

The electronic spectrum of AcMP8 at pH 10.51 (envelope e in Figure 5) shows that the hydroxo complex (HHis$-$Fe$^{3+}-$OH$^-$) exists as a mixture of $S = {}^1/_2$ and $S = {}^5/_2$ components at 25 °C. The B band is red-shifted to 399.1 nm (from 396.1 nm at pH 7.00) and exhibits a low molar absorptivity ($\epsilon_{396.1nm,pH10.51} = 9.11 \times 10^4$ M^{-1} cm^{-1}). The Q_v and Q_o bands of the $S = {}^1/_2$ state appear at 533 and 570 nm, respectively, while the CT ($b_{2u}(\pi) \rightarrow e_g(d\pi)$) band of the $S = {}^5/_2$ state is located at 600 nm and is therefore red-shifted by ~20 nm relative to the transition maximum of this band at pH 7.00. The higher energy CT band ($a_{2u}'(\pi) \rightarrow e_g(d\pi)$) of the $S = {}^5/_2$ state is normally located ~1400 cm^{-1} to the blue of the first[13b] but cannot be distinguished at pH 10.5 due to overlap with the Q_o and Q_v bands of the $S = {}^1/_2$ state. The spectrum at pH 10.5 *cannot* be simulated by mixing the spectrum of the $S = {}^5/_2$ complex at pH 7.0 with that of the predominantly $S = {}^1/_2$ complex at pH 12.8; for all combinations of mixing coefficients, the resultant envelope fails to reproduce the observed intensity at 600 nm. This clearly indicates a change in the identity of the axial ligands in the sextet species upon raising the pH to 10.5. Uno and co-workers[89a] have shown that the energy of the $b_{2u}(\pi) \rightarrow e_g(d\pi)$ CT band increases linearly with increasing pK_a of the axial alkoxide ligand in high-spin five-coordinate [Fe(OEP)]$^+$ complexes. The observed blue shift of the $S = {}^5/_2$ CT band in the visible spectrum of AcMP8 between pH 7.0 and 10.5 is therefore consistent with ionization of coordinated water and formation of the corresponding hydroxo complex (HHis$-$Fe$^{3+}-$OH$^-$).[89b]

We attribute the final pK_a for AcMP8 (p$K_6 = 12.71 \pm 0.05$) to ionization of coordinated histidine *trans* to OH$^-$ to form the $S = {}^1/_2$ histidin*ate* complex (Figure 6, Scheme 1, His$^--$Fe$^{3+}-$OH$^-$). The pK_2 values of free histidine and imidazole are 14.4 and 14.2, respectively,[90] while coordination of histidine to transition metals such as Co(II) and Cu(II) reduces the value of pK_2 to 12.5 and 11.7, in each case.[91] AcMP8 therefore exhibits a pK_a value for the HHis $\rightleftarrows$ His$^-$ equilibrium not significantly different from that expected on the basis of polarization of the ligand by the metal ion only. In heme proteins, however, the conjugate base may be further stabilized electrostatically through interaction with positively charged residues, which, in conjunction with the local dielectric constant and the type of H-bonding involving the conjugate acid, leads to a significant spread in pK_2 values: ~7.0 in soybean legHb *a*···HIm,[92] ~8.0 in *R. palustris* ferricytochrome *c*′,[93] 9.0 in *Escherichia coli* ferricytochrome *b*-562,[65] 10.34 in metMb···HIm,[94] 10.45 in *Chironomus plumosas* metHb···HIm,[95] >10.5 in the mitochondrial cytochromes *c*,[96] and >11.0 in the ferricytochromes c_3.[64] Interestingly, Othman *et al.*[97] recently attributed a pK_a of 13.3 in ferrous MP8 to ionization of the proximal histidine. The higher electron density at the metal in the Fe(II) complex, relative to *ferric* AcMP8, therefore appears to further shift the HHis $\rightleftarrows$ His$^-$ equilibrium to higher pH.

The electronic spectrum of the His$^--$Fe$^{3+}-$OH$^-$ complex at pH 12.8 (envelope f in Figure 5) is consistent with an almost pure $S = {}^1/_2$ state; residual intensity at 600 nm does however indicate the presence of some un-ionized $S = {}^5/_2$ HHis$-$Fe$^{3+}-$OH$^-$ and, possibly, a minor $S = {}^5/_2$ His$^--$Fe$^{3+}-$OH$^-$ component. The B band is further red-shifted to 405.6 nm and exhibits an increase in intensity ($\epsilon_{405.6,pH12.8} = 9.74 \times 10^4$ M^{-1} cm^{-1}). This confirms an increase in the crystal field splitting consistent with the enhanced σ-donor power of the axial ligands.

We[75] previously fitted two pK_a's to the data for MP8 in 20% methanol$-$water solution in the pH range 6$-$13; the first (8.90 $\pm$ 0.03) was assigned to ionization of iron-bound water, while the second (10.48 $\pm$ 0.09) was assigned to ionization of His-18 to form the histidin*ate* complex. The spectroscopic transition between pH 12 and 13 was ascribed to aggregation of MP8.[75] However, the near-UV spectra show no signs of aggregation, which characteristically leads to hyperchromism in the N band region and hypochromism of the B band. The present findings for AcMP8 indicate that the pK_a's for MP8[75] are probably incorrect. A refit of the data gave three alkaline pK_a's: 8.89 $\pm$ 0.02, 10.42 $\pm$ 0.04, 13.5 $\pm$ 0.6. The first and third, as for AcMP8, correspond to ionization of iron-bound water and His-18, respectively. More importantly, however, the second alkaline pK_a (10.42) is absent in AcMP8 where the α-amino group of Cys-14 has been protected by acetylation, and we therefore attribute this pK_a to deprotonation of the terminal amino group of MP8. The pK_a of the amino group of free cysteine is 10.34,[48b] suggesting that the specific microenvironment of the terminal amino group in MP8 is not particularly perturbed by the heme group or the other residues of the polypeptide chain. This result directly confirms that acetylation selectively protects the α-amino group of the heme peptide and further shows that *remote* ionization equilibria can perturb the electronic structure of the chromophore.

Stability of AcMP8 at High pH: Kinetics of μ-Oxo Dimerization. The time dependence of the electronic spectrum of AcMP8 at pH 14 (Figures S5 and S6a$-$d, Supporting Information) indicates the formation of an aggregated high-spin

(82) George, P.; Hanania, G. I. H. *Biochem. J.* **1952**, *52*, 517.
(83) Hanania, G. I. H.; Nakhleh, E. T. *Ann. N.Y. Acad. Sci.* **1975**, *244*, 35.
(84) Beetlestone, J. G.; Irvine, D. H. *J. Chem. Soc.* **1964**, 5086.
(85) Margalit, R.; Schejter, A. *Eur. J. Biochem.* **1973**, *32*, 492.
(86) George, P.; Hanania, G. I. H. *Biochem. J.* **1957**, *65*, 756.
(87) Lumry, R. In *Probes of Structure and Function of Macromolecules and Membranes*; Chance, B., Yonetani, T., Mildvan, A. S., Eds.; Academic Press: New York, 1971; Vol. 2, p 353.
(88) George, P.; Irvine, D. H.; Glauser, S. C. *Ann. N.Y. Acad. Sci.* **1960**, *88*, 393.
(89) (a) Uno, T.; Hatano, K.; Nishimura, Y.; Arata, Y. *Inorg. Chem.* **1990**, *29*, 2803. (b) Enhanced charge donation from the anionic ligand destabilizes the dπ orbitals and therefore raises the energy of the excited state $(b_{2u})^1(e_g)^3$ resulting from the charge-transfer transition. Interestingly, it has been suggested[13b] that, in the $S = {}^5/_2$ state of hydroxo metMb, the axial ligand combination HHis$-$Fe$^{3+}-$OH$^-$ is earmarked by the location of the Q_o band at 609 nm and *not* near 545 nm as in the $S = {}^5/_2$ aqua complex. Such an assignment requires a red shift of ~1930 cm^{-1} for the Q_o band, which is inconsistent with the observed *blue shift* of ~770 cm^{-1} when the axial ligand changes from phenolate (pK_a 9.89) to methoxide (pK_a 15.5) in high-spin [Fe(OEP)(L)]$^+$.[89a] We therefore suggest that a blue shift of both the Q_v and Q_o bands of the order of 770 cm^{-1} should attend ionization of bound water in metMb and that the band assigned to the (3,0) component of the Q$-$B coupled states at 476 nm[13b] more likely corresponds to the blue-shifted Q_v band of the sextet state.
(90) Yagil, G. *Tetrahedron* **1967**, *23*, 2855.
(91) Martin, R. B. *Proc. Natl. Acad. Sci. U.S.A.* **1974**, *71*, 4346.
(92) Sievers, G.; Gadsby, P. M. A.; Peterson, J.; Thomson, A. J. *Biochim. Biophys. Acta* **1983**, *742*, 637.
(93) Jackson, J. T.; La Mar, G. N.; Bartsch, R. G. *J. Biol. Chem.* **1983**, *258*, 1799.
(94) George, P.; Hanania, G. I. H.; Irvine, D. H.; Abu-Issa, I. *J. Chem. Soc.* **1964**, 5689.
(95) Mohr, P.; Scheler, W.; Schumann, H.; Muller, K. *Eur. J. Biochem.* **1967**, *3*, 158.
(96) Gadsby, P. M. A.; Peterson, J.; Foote, N.; Greenwood, C.; Thomson, A. J. *Biochem. J.* **1987**, *246*, 43.
(97) Othman, S.; Le Lirzin, A.; Desbois, A. *Biochemistry* **1993**, *32*, 9781.
(98) Osuka, A.; Maruyama, K. *J. Am. Chem. Soc.* **1988**, *110*, 4454.

($S = {}^5/_2$) product from the $S = {}^1/_2$ starting complex. The Soret band initially at 407.0 nm exhibits a marked blue shift to 394.8 nm at $t = 106$ h. This is accompanied by pronounced hyperchromism in the N band region (~340 nm) and hypochromism of the Soret band, which drops to 33% of its initial intensity. Such spectroscopic changes are *not* consistent with formation of a *simple* $\pi-\pi$ dimer in which the spin state is preserved, though they do indicate nearly parallel alignment of the heme groups and exciton coupling of the principal *xy*-polarized transition dipoles.[98] The Q_v (537.0 nm) and Q_o (564.9 nm) bands of the $S = {}^1/_2$ state decrease in intensity with increasing time, and this, in conjunction with the progressive increase in intensity of the band at ~600 nm, clearly demonstrates a time-dependent transition to the $S = {}^5/_2$ state. The visible band at ~600 nm in AcMP8···OH^- has been assigned to the charge-transfer transition ($b_{2u}(\pi) \rightarrow e_g(d\pi)$) of the *high-spin* component of the equilibrium mixture ($S = {}^1/_2 \rightleftarrows S = {}^5/_2$) and appears to reflect axial ligation by an anionic oxygen donor ligand (*vide supra*). On the basis of the similarity between the electronic spectrum of AcMP8 at pH 14 (after 106 h) and that of alkaline [Fe(PPIX)], which readily forms μ-oxo dimers as the pH is raised,[9c,99−101] and the kinetically determined orders of 2 and 0 with respect to [Fe] and [OH^-], respectively, we propose that AcMP8 undergoes slow μ-oxo dimerization at high pH (mechanism in Scheme S1). Importantly, these results demonstrate that, on the time scale of the pH titration (Figure 6), the spectroscopic changes due to μ-oxo dimerization of AcMP8 are insignificant and that the high-pH (>12) optical transition is a true ionization equilibrium rather than a spurious base-catalyzed side reaction.

pH Dependence of the Electronic Spectrum of Six-Coordinate AcMP8···3-CNPy: The Alkaline Range. We return finally to examine the unusual behavior of the 3-CNPy complex of AcMP8 in alkaline solution. The first of the alkaline pK_a's (p$K'_4 = 7.83 \pm 0.04$) for the AcMP8···3-CNPy complex (Figure 7) is attributed to ionization of His-18 to form the His^- complex depicted in Scheme 2. The value of this pK_a is now suggested to be very much lower than that in the HHis−Fe^{3+}−OH^- complex (12.71, Scheme 1) due to the strong π-acceptor capacity[77] and low σ-basicity of the 3-CNPy ligand coordinated *trans* to the ionizing histidine ligand. Electrostatic stabilization of the conjugate base is normally proposed to account for depression of this pK_a in heme proteins.[64] In the present case, however, we suggest that M $d\pi \rightarrow$ pyridine $p\pi$ back-donation acts as an efficient electron sink for the increase in axial σ- and π-electron density attending ionization of the *trans* histidine ligand, thereby stabilizing the histidin*ate* complex.

The electronic spectrum at pH 9.00 (Figures 8) shows that the spin distribution of the complex changes during this equilibrium. The Q_o (552.8 nm) and Q_v (522.5 nm) bands of the $S = {}^1/_2$ state decrease in intensity, while the CT band (622 nm at pH 6.60, $b_{2u}(\pi) \rightarrow e_g(d\pi)$) increases in intensity and shifts to 609.5 nm at pH 9.00. The Q_v band of the $S = {}^5/_2$ component appears as a shoulder at 489.1 nm at pH 9.00, while the B band drops slightly in intensity (7%) and exhibits a small blue shift to 399.9 nm from 400.7 nm at pH 6.60. The spectroscopic changes are accompanied by well-defined isosbestic points at 410, 528, and 550 nm and are consistent with formation of a new complex also existing as a $S = {}^1/_2 \rightleftarrows S = {}^5/_2$ mixture. The increase in intensity and 12.6 nm blue shift of the $S = {}^5/_2$ CT band suggest formation of the His^- complex in which the Fe−$N_{imidazolate}$ distance might be considerably shorter than the Fe−$N_{imidazole}$ distance in the pH 6.60 complex.[102] Concomitant weakening of the *trans* Fe−$N_{3\text{-CNPy}}$ bond could cause a small out-of-plane displacement of the Fe(III) ion toward the anionic ligand and hence account for the observed increase in the $S = {}^5/_2$ component as the pH is raised from 6.60 to 9.00. The blue-shifted CT band ($b_{2u}(\pi) \rightarrow e_g(d\pi)$) of the high-spin component at pH 9.00 reflects destabilization of the $d\pi$ orbitals of the Fe(III) ion due to enhanced electron−electron repulsion brought about by symmetry-allowed mixing of the $p\pi$ MO with large amplitude on the donor nitrogen of the imidazol*ate* ligand with the half-filled $d\pi$ orbital of the metal.

The second alkaline pK_a (p$K'_5 = 10.13 \pm 0.01$) of the AcMP8/3-CNPy system (Figure 7) does *not* involve the formation of a μ-oxo dimer since (i) the B to N band intensity ratio and the shape of the near-UV absorption envelope in Figure 8a do not match those found for the AcMP8 $\pi-\pi$ dimer (see part 2) or those of the μ-oxo dimer at high pH (Figure S6c,e), and (ii) the pH 9−12 optical transition could not be fitted to any pH-dependent dimerization model.

Since the data are well-fitted by eq 9, treating consecutive single-proton ionization equilibria of related monomeric species, we suggest that the optical transition (p$K'_5 = 10.13$) involves an axial ligand interchange process wherein His^- is replaced by OH^- (Scheme 2). Although hydroxide ion carries a higher donor atom charge than His^-, it is a weaker σ-donor and may be expected to shift the spin distribution of the sample toward the $S = {}^5/_2$ state, especially if it is coordinated *trans* to a weak σ-donor such as 3-CNPy. This assignment is supported by the fact that the pH 11.8 spectrum of the AcMP8/3-CNPy system (Figure 8) differs significantly from that of AcMP8 in the absence of 3-CNPy at pH 10.5 (Figure 5); the species formed at pH 11.8 in the AcMP8/3-CNPy system is *predominantly high-spin*. Thus, the Q_o (552.8 nm) and Q_v (522.5 nm) bands of the $S = {}^1/_2$ state at pH 9.0 are virtually absent from the visible spectrum at pH 11.8 (Figure 8b), while the Soret band is of much lower intensity ($\epsilon_{399.2\text{nm,pH11.8}} = 7.13 \times 10^4\ M^{-1}\ cm^{-1}$) relative to that at pH 9.0 ($\epsilon_{399.9\text{nm,pH9.0}} = 1.08 \times 10^5\ M^{-1}\ cm^{-1}$). Furthermore, the $b_{2u}(\pi) \rightarrow e_g(d\pi)$ (599.8 nm) and $a_{2u}'(\pi) \rightarrow e_g(d\pi)$ (567.3 nm) CT bands that signal axial ligation by an O^- donor in the $S = {}^5/_2$ state[89a] and produce the distinctive olive-green color of the solution dominate the visible spectrum of the AcMP8/3-CNPy system at pH 11.8 (Figure 8b). The spectra clearly indicate that the second alkaline transition in the presence of 3-CNPy does not generate the low-spin His^-−Fe^{3+}−OH^- complex. We therefore suggest that His^- is replaced by OH^- (Scheme 2) and that this transition to weaker axial ligation at the metal (3-CNPy−Fe^{3+}−OH^-) effects the observed shift to the $S = {}^5/_2$ configuration.

The diminished intensity of the Soret band for the 3-CNPy−Fe^{3+}−OH^- complex (Figure 8a) is similar to that observed on formation of the HHis−Fe^{3+}−OH^- complex at pH 10.5 (Figure

(99) Bell, S. E. J.; Hester, R. E.; Hill, J. N.; Shawcross, D. R.; Smith, J. R. L. *J. Chem. Soc., Faraday Trans.* **1990**, *86*, 4017.
(100) Sutter, J. R.; Hambright, P.; Chock, P. B.; Krishnamurthy, M. *Inorg. Chem.* **1974**, *13*, 2764.
(101) Fleischer, E. B.; Palmer, J. M.; Srivastava, T. S.; Chatterjee, A. *J. Am. Chem. Soc.* **1971**, *93*, 3162.

(102) (a) The suggestion that the axial Fe−N bonds may not be equivalent in the pH 9.00 complex is supported by the observation that the mean M−N distance to the imidazolate ligands in [Fe(TPP)(4(5)-Me-$Im^-)_2]^+$ is 1.943(21) Å,[102b] while the axial M−L bonds in the planar low-spin 3-chloropyridine complex [Fe(OEP)(3-$ClPy)_2]^+$ are considerably longer at 2.031(2) Å and still longer in the $S = {}^5/_2$ state at 2.194(2) Å.[74] In the S_4-ruffled $S = {}^1/_2$ complexes [Fe(TMP)(4-$CNPy)_2]^+$ [77b] and [Fe(TPP)$(Py)_2]^+$,[102c] the mean axial Fe−N distances are 2.011(8) Å and 2.003(7) Å, respectively. Thus the larger steric bulk and lower σ-basicity of a pyridine relative to an imidazol*ate* ligand will always lead to a longer axial Fe−N distance, irrespective of the conformation of the porphyrin core or the electronic structure of the pyridine ligand. (b) Quinn, R.; Strouse, C. E.; Valentine, J. S. *Inorg. Chem.* **1983**, *22*, 3934. (c) Inniss, D.; Soltis, S. M.; Strouse, C. E. *J. Am. Chem. Soc.* **1988**, *110*, 5644.

5a), although the observed hypochromism in the former case is more difficult to understand as the system is changing from mainly $S = {}^1/_2$ to mainly $S = {}^5/_2$, a situation that should lead to enhanced intensity of the Soret band. However, asymmetric axial ligation in a six-coordinate $S = {}^5/_2$ mixed-ligand complex might lead to out-of-plane displacement of the metal toward one axial ligand, thereby favoring a more square pyramidal coordination geometry. Since five-coordinate $S = {}^5/_2$ ferric heme proteins exhibit less intense Soret bands than their high-spin six-coordinate analogs,[33] the present spectroscopic data seem to suggest distinct axial asymmetry in the 3-CNPy−Fe^{3+}−OH^- complex. With hydroxide coordinated *trans* to a weak σ-donor such as 3-CNPy, the d_{z^2} electron of the high-spin ion could be localized on the 3-CNPy side of the metal by d_{z^2}–$4p_z$ hybridization,[103] which would tend to enhance the axial L−M antibonding interaction and thus impart increased five-coordinate character to the complex. However, a true five-coordinate hydroxo complex in which 3-CNPy has been lost due to extreme elongation of the $Fe-N_{3\text{-CNPy}}$ bond is *not* formed since the spectrum is inconsistent with that of [Fe(PPIXDME)(OH^-)].[104]

The final far alkaline optical transition of the AcMP8/3-CNPy system ($pK'_6 = 13.9 \pm 0.1$, Figure 7) is not completely covered by the electronic spectrum recorded at pH 13.4 (Figures 8), but from the observed changes relative to the pH 11.8 spectrum it is possible to infer that the spin equilibrium exhibits a reverse shift toward the $S = {}^1/_2$ state at very high pH. Thus the Soret band, while dropping somewhat in intensity, displays a discrete red shift of 4.5 nm to 403.7 nm at pH 13.4, consistent with an increase in the axial ligand field strength. The intensity of the $b_{2u}(\pi) \rightarrow e_g(d\pi)$ CT band of the $S = {}^5/_2$ state decreases by 27% on raising the pH to 13.4. The band therefore reduces to a shoulder at 602.4 nm. The $a_{2u}'(\pi) \rightarrow e_g(d\pi)$ CT band of the high-spin state formerly at 567.3 nm at pH 11.8 *appears* not to change significantly with the increase in pH to 13.4, but this is a consequence of overlap with the Q_o band of the low-spin state which increases in intensity as the pH is raised. Since the Q_v band is the (1,0) vibronic component of the Q_o band, an increase in the intensity of the latter should be accompanied by the appearance of the former at $\sim$1076 cm^{-1} to the blue of 567 nm.[105] This is confirmed by the appearance of the band at 537.7 nm in the pH 13.4 spectrum. We therefore propose (Scheme 2) that at pH >13, 3-CNPy is replaced by OH^- and that the bis(hydroxo) complex formed is predominantly *low-spin*. This is supported by the EPR, resonance Raman, and optical data of Spiro *et al.*,[103,106a] which demonstrate that the bis(hydroxo) complex of $[Fe(TMPyP)]^{5+}$ obtained at high pH exists as a thermal spin-equilibrium mixture of $S = {}^1/_2$ and $S = {}^5/_2$ components.[106b]

The Possibility of a Pure Intermediate-Spin ($S = {}^3/_2$) State for AcMP8. The present study has shown that AcMP8 exists as a *six-coordinate complex* with pH-dependent changes in axial ligation over the *full pH range* from $\sim$1.8 to >13. At pH 7.00 (25 °C), our spectroscopic data are consistent with a predominantly high-spin ($S = {}^5/_2$) component in equilibrium with a minor $S = {}^1/_2$ component, and our axial ligand assignment is HHis−Fe^{3+}−OH_2. However, at pH 10.5 (25 °C), the visible spectrum of the hydroxo complex (HHis−Fe^{3+}−OH^-) indicates that the populations of the $S = {}^5/_2$ and $S = {}^1/_2$ components are about equal, while at pH 12.8, the His^-−Fe^{3+}−OH^- complex is predominantly low-spin and is in equilibrium with a minor $S = {}^5/_2$ component.

Our interpretation of the pH-dependent species distribution of AcMP8 in aqueous solution therefore differs from that proposed by Wang *et al.*,[39] particularly in the neutral and alkaline regions. First, Wang *et al.*[39] suggest that, at pH 7, AcMP8 exists as the six-coordinate complex with water and histidine as axial ligands (HHis−Fe^{3+}−OH_2) and that this complex is a *thermal* equilibrium mixture of *pure* $S = {}^5/_2$ and $S = {}^3/_2$ components. We agree with their axial ligand assignment but do not agree that the system represents a thermal $S = {}^5/_2 \rightleftarrows S = {}^3/_2$ equilibrium for two reasons. (i) The EPR spectrum of AcMP8···OH_2 recorded by Wang *et al.*[39] at 11 K exhibits g values of 5.8 ($g_\perp$) and 2.0 ($g_\parallel$), appropriate for a tetragonal quantum-mechanically admixed intermediate-spin species ($S = {}^3/_2, {}^5/_2$) with a ground state wave function comprising 90% $^6A_1$ and 10% $^4A_2$ character.[41c] Thus, their "high-spin" component is not a pure $^6A_1$ species, although it is *predominantly* high-spin. (ii) A *pure* $S = {}^3/_2$ iron(III) porphyrin with tetragonal symmetry should exhibit g values of 4.0 ($g_\perp$) and 2.0 ($g_\parallel$).[16,107−109] If AcMP8···OH_2 is in thermal equilibrium between $S = {}^5/_2$ and $S = {}^3/_2$ states, as suggested by Wang *et al.*,[39] then the EPR spectrum should exhibit three observable signals with $g_\perp = 6.0$ ($S = {}^5/_2$), $g_\perp' = 4.0$ ($S = {}^3/_2$), and two overlapping signals at $g = 2.0$ ($g_\parallel$ from the $S = {}^5/_2$ component and $g_\parallel'$ from the $S = {}^3/_2$ component). However, since *no* signal at $g = 4.0$ is present in the EPR spectrum of AcMP8···OH_2,[39] their conclusion that a *pure* $S = {}^3/_2$ component is present at pH 7 is inconsistent with the EPR data. In fact, the suggestion of Wang *et al.*[39] that the reduced amplitude of the EPR signals of AcMP8···OH_2 relative to those of AcMP8···F^- reflects the presence of an EPR-silent $S = {}^3/_2$ complex is questionable, particularly since the intensities of the EPR signals of hemoproteins[110] and heme peptides[27,28,41c] are known to vary as a result of sample-dependent spin−lattice relaxation effects.[111]

We consider it to be unlikely that an iron(III) porphyrin with three unpaired spins (i.e., a $S = {}^3/_2$ species) will be EPR-silent at 11 K, except in the (as yet undocumented) case of a dimer comprising two antiferromagnetically coupled $S = {}^3/_2$ heme centers. In fact, our EPR and Mössbauer[112] study on AcMP8 in part 3[41c] demonstrates that the neutral and alkaline complexes of AcMP8 are thermal equilibrium mixtures of $S = {}^3/_2, {}^5/_2$ and $S = {}^1/_2$ components, a conclusion that is further supported by our magnetic susceptibility measurements in part 4.[41d] Indeed, a *pure* $S = {}^3/_2$ iron(III) porphyrin (100% $^4A_2$ ground state wave function) has yet to be isolated,[41c] presumably because it is difficult to achieve a vanishing axial ligand field—particularly in aqueous solution.[113]

However, it is not necessary to resort to EPR measurements to exclude the possibility that AcMP8 populates a pure $S = {}^3/_2$

(103) Reed, R. A.; Rodgers, K. R.; Kushmeider, K.; Spiro, T. G.; Su, Y. O. *Inorg. Chem.* **1990**, *29*, 2881.
(104) Yoshimura, T.; Ozaki, T. *Arch. Biochem. Biophys.* **1984**, *230*, 466.
(105) 1076 cm^{-1} is the vibrational quantum[13b] separating the (1,0) and (0,0) components of the Q−B coupled states in an $S = {}^1/_2$ system such as His^-−Fe^{3+}−OH^-.
(106) (a) Rodgers, K. R.; Reed, R. A.; Spiro, T. G.; Su, Y. O. *New J. Chem.* **1992**, *16*, 533. (b) The spectroscopic changes of the AcMP8/3-CNPy system in the visible region that attend the increase in pH from 9.0 to 11.8 are analogous to the spectroscopic changes of the $S = {}^5/_2 \rightleftarrows S = {}^1/_2$ $[Fe(TMPyP)(OH)_2]^{3+}$ complex as the temperature is lowered from 100 to 10 °C;[106a] the fractional population of the $S = {}^1/_2$ state progressively increases. This is earmarked by the disappearance of the $b_{2u}(\pi) \rightarrow e_g(d\pi)$ CT band near 600 nm and a concomitant increase in the Q_o band intensity around 550 nm.[106a] The bis(hydroxo) complexes of AcMP8 and $[Fe(TMPyP)]^{5+}$ are therefore predominantly low-spin at 25 °C.
(107) Maltempo, M. M. *J. Chem. Phys.* **1974**, *61*, 2540.
(108) Maltempo, M. M.; Moss, T. H. *Q. Rev. Biophys.* **1976**, *9*, 181.
(109) Shelly, K.; Bartczak, T.; Scheidt, W. R.; Reed, C. A. *Inorg. Chem.* **1985**, *24*, 4325.
(110) Yonetani, T.; Schleyer, H. *J. Biol. Chem.* **1967**, *242*, 3926−3933.
(111) Drago, R. S. *Physical Methods for Chemists*, 2nd ed.; Saunders College Publishing: Orlando, FL, 1992; p 394.
(112) Munro, O. Q.; Marques, H. M.; Pollak, H.; Malas, N. *Nucl. Instrum. Methods Phys. Res.* **1993**, *B76*, 315.

state in solution at 25 °C. The visible CT bands of AcMP8···OH_2 (pH 7) may be used to establish that states with >50% $^4A_2$ character are indeed absent. Analysis of the visible spectrum of [Fe(TPP)($FSbF_5$)][109] in toluene solution, a complex whose ground state wave function comprises 75% $^4A_2$ and 25% $^6A_1$ character at 11 K, shows that the CT bands are diagnostic of this spin-mixed state. The $b_{2u}(\pi) \rightarrow e_g(d\pi)$ transition is observed at 665 nm, while the $a_{2u}'(\pi) \rightarrow e_g(d\pi)$ transition is found at 632 nm. The energy of the $b_{2u}(\pi) \rightarrow e_g(d\pi)$ transition therefore lies between that appropriate for $S = {}^1/_2$ systems (1000−1700 nm)[50] and that found in high-spin complexes of, for example, metMb (628 ± 16 nm).[114] Reference to the pH ≤10.5 electronic spectra of AcMP8 (Figure 5b) indicates that the $b_{2u}(\pi) \rightarrow e_g(d\pi)$ transition is *not* observed at wavelengths longer than 620 nm. Thus, the pH-dependent species of AcMP8 (pH ≤ 10.5) are predominantly *high-spin*; *no* evidence for components with > 50% $^4A_2$ character exists, and we therefore conclude, in contrast to Wang *et al.*,[39] that a predominantly $S = {}^3/_2$ state is *inaccessible* in aqueous solution.

The second important difference between our analysis and that of Wang *et al.*[39] concerns the first alkaline transition of the heme peptide. These authors suggest that a five-coordinate complex is formed at pH 10 as a result of ionization of iron-bound histidine ($pK_a \sim 9$) and concomitant dissociation of the *trans* ligand (H_2O). Not only do our data indicate that this transition corresponds to the ionization of *iron-bound water*, consistent with several studies on hemoproteins[79−83] and microperoxidases,[75] but we find, in accord with others,[104] that the axial histidine ionizes to form the histidinate complex at pH >12. Indeed, axial ligation by a single *sterically unhindered* imidazole produces five-coordinate complexes in aqueous solution, but only in the ferrous state.[60b,97] Five-coordinate imidazole complexes of *ferric* porphyrins are normally only encountered when access to the metal is severely restricted, due to either steric hindrance in the ligand or encumbrance of the *trans* ligation site, as in the cytochromes *c*′.[115,116] It is therefore unlikely that AcMP8 would lose water to form the five-coordinate histidinate complex, as proposed by Wang *et al.*,[39] particularly in aqueous solution.

Conclusions

The more important conclusions that can be drawn from this study are the following. (1) AcMP8 remains six-coordinate over the whole pH range in aqueous solution. (2) The axial ligand combination is critically dependent on pH. (3) While weak-field ligands favor a predominantly $S = {}^5/_2$ state, intermediate- to strong-field ligands enable population of the $S = {}^1/_2$ state. Several complexes of AcMP8, for example AcMP8···3CNPy and AcMP8···OH^-, therefore exhibit spin equilibria between the $S = {}^5/_2$ and $S = {}^1/_2$ states. (4) A *pure* $S = {}^3/_2$ state is *not* populated by AcMP8 in aqueous solution. (5) Protection of the Cys-14 α-NH_2 group of AcMP8 restricts intermolecular interaction to the formation of π-stacked complexes, thereby abolishing intermolecular coordination and considerably simplifying the number of species in solution.

Acknowledgment. We are indebted to the University of the Witwatersrand and the Foundation for Research Development for financial support and to AECI Ltd. for a postgraduate fellowship to O.Q.M.

Supporting Information Available: Figures S1 and S2 (four- and five-pK_a fits, respectively, of the variation of the Soret absorbance (397.2 nm) with pH for a 3.1 μM aqueous solution of AcMP8 at 25 °C), Figure S3 (plots of the residual absorbance (397.2 nm) as a function of pH for the fits of the spectroscopic data given in Figures 6, S1, and S2 to eq 9), Figure S4 (van't Hoff isochore for the ionization equilibrium of iron-bound water (pK_{H_2O}) in AcMP8), Figures S5 and S6 (fit of the change in concentration of pH 14.0 AcMP8 with time at 25 °C and accompanying time-dependent changes in the visible and near-UV spectra, respectively), Scheme S1 (proposed mechanism for the μ-oxo dimerization of AcMP8 at high pH), and derivation of an equilibrium model to describe the variation in total absorbance with concentration for a self-dimerizing system (eq 2) (13 pages). Ordering information is given on any current masthead page.

IC9502842

(113) Scheidt, W. R.; Reed, C. A. *Chem. Rev.* **1981**, *81*, 543.
(114) Smith, D. W.; Williams, R. J. P. *Biochem. J.* **1968**, *110*, 297.
(115) Weber, P. C.; Howard, A.; Xuong, N. H.; Salemme, F. R. *J. Mol. Biol.* **1981**, *153*, 399.
(116) Finzel, B. C.; Weber, P. C.; Hardman, K. D.; Salemme, F. R. *J. Mol. Biol.* **1985**, *186*, 627.